bioRxiv preprint doi: https://doi.org/10.1101/2021.04.11.439248; this version posted April 12, 2021. The copyright holder for this preprint (which was not certified by peer review) is the author/funder, who has granted bioRxiv a license to display the preprint in perpetuity. It is made available under aCC-BY 4.0 International license.

Experiment level curation identifies high confidence transcriptional regulatory interactions in neurodevelopment

Eric Ching-Pan Chu[1,2,3], Alexander Morin[1,2,3], Tak Hou Calvin Chang[1], Tue Nguyen[1], Yi-Cheng Tsai[1], Aman Sharma[1], Chao Chun Liu[1], Paul Pavlidis[1,2]

1. Michael Smith Laboratories, University of British Columbia, Vancouver, BC Canada
2. Department of Psychiatry, University of British Columbia, Vancouver, BC, Canada
3. Graduate Program in Bioinformatics, University of British Columbia, Vancouver, BC, Canada

*Corresponding author:
Paul Pavlidis
177 Michael Smith Laboratories
2185 East Mall
University of British Columbia
Vancouver BC V6T1Z4
Canada
604 827 4157
paul@msl.ubc.ca

bioRxiv preprint doi: https://doi.org/10.1101/2021.04.11.439248; this version posted April 12, 2021. The copyright holder for this preprint (which was not certified by peer review) is the author/funder, who has granted bioRxiv a license to display the preprint in perpetuity. It is made available under aCC-BY 4.0 International license.

Abstract

To facilitate the development of large-scale transcriptional regulatory networks (TRNs) that may enable in-silico analyses of disease mechanisms, a reliable catalogue of experimentally verified direct transcriptional regulatory interactions (DTRIs) is needed for training and validation. There has been a long history of using low-throughput experiments to validate single DTRIs. Therefore, we hypothesize that a reliable set of DTRIs could be produced by curating the published literature for such evidence. In our survey of previous curation efforts, we identified the lack of details about the quantity and the types of experimental evidence to be a major gap, despite the importance of such details for the identification of bona fide DTRIs. We developed a curation protocol to inspect the published literature for support of DTRIs at the experiment level, focusing on genes important to the development of the mammalian nervous system. We sought to record three types of low-throughput experiments: Transcription factor (TF) perturbation, TF-DNA binding, and TF-reporter assays. Using this protocol, we examined a total of 1,310 papers to assemble a collection of 1,499 unique DTRIs, involving 251 TFs and 825 target genes, many of which were not reported in any other DTRI resource. The majority of DTRIs (965, 64%) were supported by two or more types of experimental evidence and 27% were supported by all three. Of the DTRIs with all three types of evidence, 170 had been tested using primary tissues or cells and 44 had been tested directly in the central nervous system. We used our resource to document research biases among reports towards a small number of well-studied TFs. To demonstrate a use case for this resource, we compared our curation to a previously published high-throughput perturbation screen and found significant enrichment of the curated targets among genes differentially expressed in the developing brain in response to Pax6 deletion. This study

bioRxiv preprint doi: https://doi.org/10.1101/2021.04.11.439248; this version posted April 12, 2021. The copyright holder for this preprint (which was not certified by peer review) is the author/funder, who has granted bioRxiv a license to display the preprint in perpetuity. It is made available under aCC-BY 4.0 International license.

43 demonstrates a proof-of-concept for the assembly of a high confidence DTRI resource in order to
44 support the development of large-scale TRNs.

45 Author Summary

46 The capacity to computationally reconstruct gene regulatory networks using large-scale
47 biological data is currently limited by the absence of a high confidence set of one-to-one
48 regulatory interactions. Given the lengthy history of using small scale experimental assays to
49 investigate individual interactions, we hypothesize that a reliable collection of gene regulatory
50 interactions could be compiled by systematically inspecting the published literature. To this end,
51 we developed a curation protocol to examine and record evidence of regulatory interactions at
52 the individual experiment level. Focusing on the area of brain development, we applied our
53 pipeline to 1,310 publications. We identified 3,601 individual experiments, providing detailed
54 information about 1,499 regulatory interactions. Many of these interactions have verified activity
55 specifically in the embryonic brain. By capturing reports of regulatory interactions at this level of
56 granularity, we present a resource that is more interpretable than other similar resources.

57 Introduction

58 Reconstruction of transcriptional regulatory networks (TRNs) has the potential to enable
59 in-silico analysis of developmental processes and disease mechanisms. As such, using high-
60 throughput biological data to infer large scale TRNs is an area under active research; recent
61 examples include (1–4). However, the utility of these TRNs has been hindered by the absence of
62 a high confidence set of regulatory interactions for training and validation. Researchers have
63 historically used less scalable experimental techniques to investigate direct transcriptional
64 regulatory interactions (DTRIs). While low-throughput, such methods tend to be considered

bioRxiv preprint doi: https://doi.org/10.1101/2021.04.11.439248; this version posted April 12, 2021. The copyright holder for this preprint (which was not certified by peer review) is the author/funder, who has granted bioRxiv a license to display the preprint in perpetuity. It is made available under aCC-BY 4.0 International license.

65 reliable, especially if there are multiple independent lines of evidence supporting a DTRI. Thus,
66 there would be value in having resources that aggregate high-quality reports of DTRIs, forming
67 the topic of the current work. Our particular interest is in DTRIs of relevance to the developing
68 nervous system, as mutations in transcription factor (TF) genes (5–7) and regulatory regions (8–
69 10) have been highly implicated in neurodevelopmental disorders.

70 We define DTRIs as pairwise interactions between a transcription factor (TF) and a target
71 gene where the TF modulates target expression by physically binding to a cis-regulatory element
72 (cRE). There are three types of low-throughput experimental paradigms commonly used to
73 elucidate DTRIs, including TF perturbation, TF-DNA binding, and TF-reporter assays (Fig 1A).
74 In TF perturbation assays, manipulation of TF expression is followed by an assessment of target
75 gene expression. In TF-DNA binding assays, protein-DNA interactions between the TF and the
76 cRE are evaluated. Finally, TF-reporter assays measure the functional impact of the TF binding
77 on the associated cRE sequence. While low-throughput assays are not infallible, they generally
78 yield higher confidence than high-throughput alternatives by evading the need for large scale
79 inferential statistics and enabling detailed and readily replicable characterization of single
80 DTRIs; examples: (11,12) (Fig 1B). Notably, such low-throughput experiments are routinely
81 used to validate putative targets identified by more scalable approaches. Given the importance
82 and wide acceptance of these types of evidence, it would be useful to assemble a centralized
83 catalogue of DTRIs that is supported by low-throughput experimental evidence in the published
84 literature.

85 There have been a number of earlier efforts to aggregate DTRIs from the literature:
86 ENdb: (13), TRRUST: (14,15), CytReg: (16), OReganno: (17–19), HTRIdb: (20), TFe: (21),
87 TFactS: (22), InnateDB: (23). None of these curation efforts were tailored to the

bioRxiv preprint doi: https://doi.org/10.1101/2021.04.11.439248; this version posted April 12, 2021. The copyright holder for this preprint (which was not certified by peer review) is the author/funder, who has granted bioRxiv a license to display the preprint in perpetuity. It is made available under aCC-BY 4.0 International license.

neurodevelopment context. More importantly, these studies generally record annotations of pairs of interacting genes but capture little information about the underlying experimental evidence. This is notable because the type and quantity of evidence is expected to affect the reliability of a reported interaction. Specifically, each individual type of evidence provides only a limited view of any given DTRI. TF perturbation assays enable the assessment of the TF's ability to modulate target gene expression but cannot decipher its functional dependence on direct physical binding. Likewise, while TF binding at a cRE is necessary for regulation, detection of TF-DNA binding alone is insufficient for demonstrating functional activity. TF-reporter assays simultaneously demonstrate both functional modulation and physical binding but often by examining the given DTRI outside of the native genomic and cellular context. As such, integration across these types of experiments should help establish DTRIs with high confidence.

We hypothesize that curation of details at the individual experiment level would facilitate identification of bona fide DTRIs. In this study, we undertook a systematic effort to curate the literature at a high level of detail. Consequently, we present a resource that is highly interpretable and more suitable for the evaluation of high-throughput predictions than other similar resources. Finally, our curation effort provides a partial summary snapshot of the literature landscape surrounding transcriptional regulation in the developing brain.

bioRxiv preprint doi: https://doi.org/10.1101/2021.04.11.439248; this version posted April 12, 2021. The copyright holder for this preprint (which was not certified by peer review) is the author/funder, who has granted bioRxiv a license to display the preprint in perpetuity. It is made available under aCC-BY 4.0 International license.

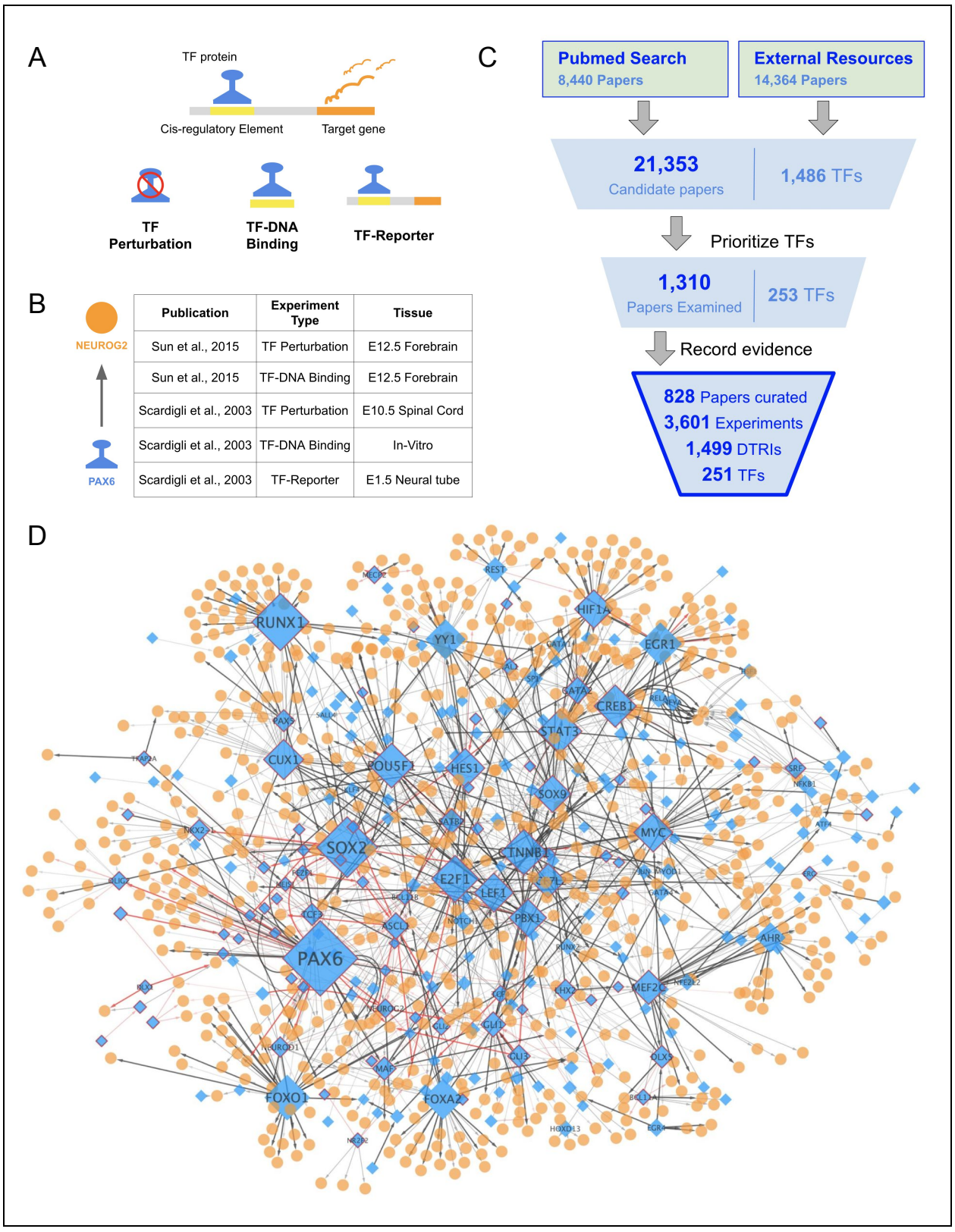

Publication	Experiment Type	Tissue
Sun et al., 2015	TF Perturbation	E12.5 Forebrain
Sun et al., 2015	TF-DNA Binding	E12.5 Forebrain
Scardigli et al., 2003	TF Perturbation	E10.5 Spinal Cord
Scardigli et al., 2003	TF-DNA Binding	In-Vitro
Scardigli et al., 2003	TF-Reporter	E1.5 Neural tube

Fig 1. Summary of curation.

bioRxiv preprint doi: https://doi.org/10.1101/2021.04.11.439248; this version posted April 12, 2021. The copyright holder for this preprint (which was not certified by peer review) is the author/funder, who has granted bioRxiv a license to display the preprint in perpetuity. It is made available under aCC-BY 4.0 International license.

(A) A schematic of the three types of low-throughput experimental evidence we considered. (B) Curated records for the interaction between PAX6 and NEUROG2 provided as an example. (C) Overall curation workflow. The count of papers and the corresponding number of TFs in each stage of curation are printed. Summary statistics of the final curation output are displayed at the bottom (D) The manually curated regulatory network. TFs are diamond shaped and colored blue. Targets are circles and colored orange. The sizes of TFs correspond to the number of targets. TFs with 10 or more targets are labeled with the official HGNC gene symbol. Edge transparency corresponds to the number of types of experiments. Red edges represent DTRIs with experimental validation in primary CNS tissues or cells. Only the largest network component with 946 nodes and 1481 edges is displayed.

Results

Overview of curation

Our curation pipeline is summarized in Fig 1C (see Methods for details). Briefly, for each TF, we assembled a set of candidate papers (S. Table S1). Next, we manually prioritized TFs for curation based on annotated associations with central nervous system (CNS) development and the number of candidate papers retrieved (S. Table S2). For each paper examined, we recorded the details of all reported experiments that lend support to any DTRI in humans or mice (Table 1, S. Table S3). For reporting, we mapped all genes to human orthologs while retaining the species information as an additional feature. Applying this pipeline to a total of 1,310 papers, we established a collection of 1,499 unique DTRIs, involving 251 TFs and 825 targets, from 828 papers. This manually curated network is displayed in Figure 1D and the complete set of curated interactions are provided in S. Table S4. In the following sections, we present a detailed summary of the curated data resource and compare it to a high-throughput TF perturbation screen.

Experiment Type	One of three types of experiment being curated. *Value: TF Perturbation, TF-DNA Binding, or TF-Reporter.*

bioRxiv preprint doi: https://doi.org/10.1101/2021.04.11.439248; this version posted April 12, 2021. The copyright holder for this preprint (which was not certified by peer review) is the author/funder, who has granted bioRxiv a license to display the preprint in perpetuity. It is made available under aCC-BY 4.0 International license.

Context Type	A broad classification of the cellular context tested. *Value: Primary Tissue, Primary Cells, Cell Line, or In-Vitro.*
Cell Type	An ontology term that best corresponds to the tissue or cell type used. *Example: UBERON:0001017 (central nervous system)*
TF Species	The species of the TF protein or sequence. *Value: Human or Mouse.*
Target Species	The species of the target protein or regulatory element. *Value: Human or Mouse.*
TFBS Position	A broad classification of the distance between the transcription factor binding site (TFBS) and the target transcription start site (TSS). *Value: Proximal or Distal.*
Mode	The mode or direction of regulation. *Value: Activation or Repression.*
[1]Details	**TF Perturbation** Effect: *Knock Out, Knock Down or Overexpression* [2]Type: *Constitutive or Induced* **TF-DNA Binding** Method: *ChIP-assay or EMSA (Electrophoretic Mobility Shift Assay)* [3]TF Source Type: *Primary Tissue, Primary Cells, or Cell Line* **TF-Reporter** Mutated: *TRUE or FALSE* [4]Binding Verified: *Putative, EMSA, or None*

Table 1. Experimental details recorded during curation.

[1]Different sets of details are recorded for different types of experiments. [2]Constitutive perturbation refers to mutations that are present throughout the course of development, as opposed to induced perturbations using Cre-loxP or RNA interference that are triggered closer to the time of assay. [3]The TF protein used in EMSA experiments may be sourced differently across experiments. In many cases, it is obtained from cell lines after TF transfection. In other cases, the endogenous protein is obtained directly from primary tissues or cells. [4]For TF-reporter assays where the cRE sequence is mutated and tested, the impact of the mutation on TF-DNA binding is sometimes verified using additional EMSA experiments.

bioRxiv preprint doi: https://doi.org/10.1101/2021.04.11.439248; this version posted April 12, 2021. The copyright holder for this preprint (which was not certified by peer review) is the author/funder, who has granted bioRxiv a license to display the preprint in perpetuity. It is made available under aCC-BY 4.0 International license.

Identification of candidate papers highlights biases in TF coverage

The input to our curation was a corpus of candidate publications. To establish this corpus, we started by taking advantage of previous curation efforts. We obtained 14,364 papers from seven external resources, covering 1,305 TFs Fig 2A, S. Table S1). TRRUST, the largest database of literature curated DTRIs, provided more than 10,000 publications but only recovered about ~20% of those recorded in the other resources (Fig 2B, 2C). Further, overlaps among the other resources are generally small (0%-22%). These observations suggest that there may be additional papers in the literature containing reports of DTRIs. As such, we expanded the pool of candidate papers by searching PubMed using several relevant Medical Subject Headings (MeSH) terms (see Methods for details). We identified an additional set of 6,989 candidate papers for 1,140 TFs (Fig 2A). In particular, for TFs directly associated with CNS development, we were able to increase the total number of candidate papers from 5,729 to 9,839. Together, we assembled a set of 21,353 candidate papers covering 1,486 TFs.

bioRxiv preprint doi: https://doi.org/10.1101/2021.04.11.439248; this version posted April 12, 2021. The copyright holder for this preprint (which was not certified by peer review) is the author/funder, who has granted bioRxiv a license to display the preprint in perpetuity. It is made available under aCC-BY 4.0 International license.

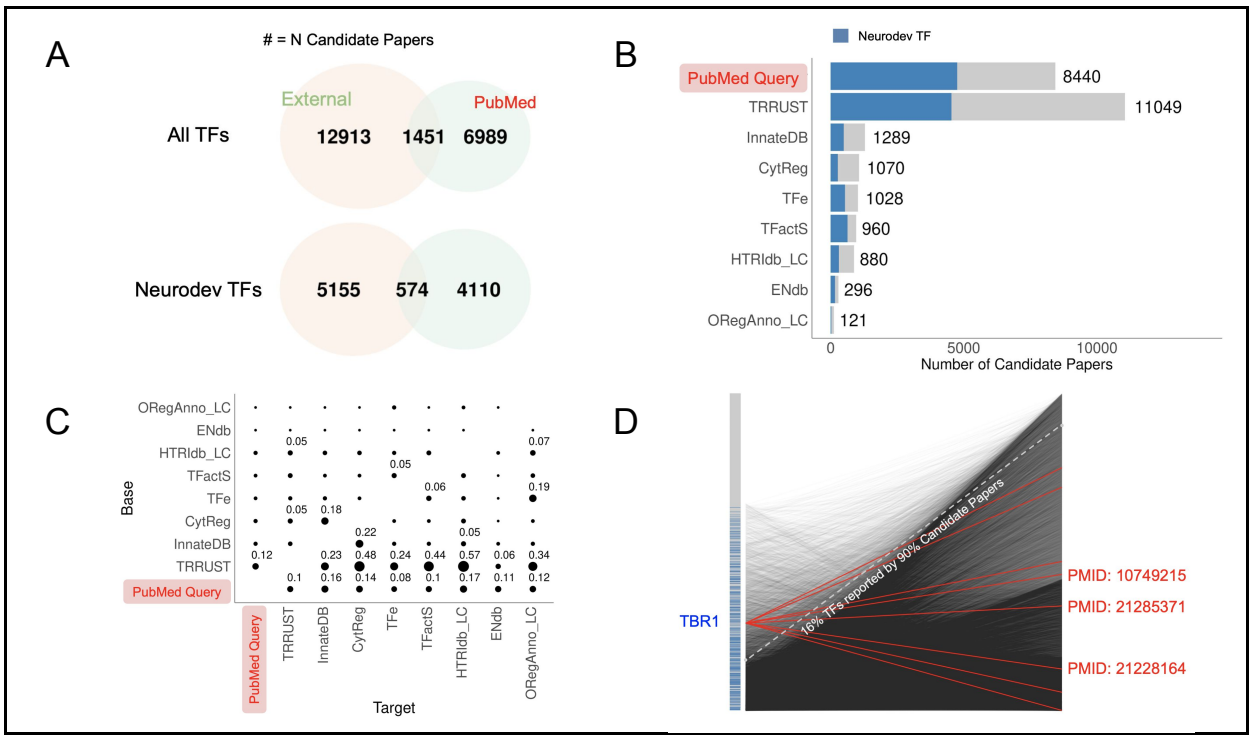

Fig 2. Overview of the candidate literature corpus.

(A) Venn diagrams showing the overlap between candidate papers sourced from external data resources versus our independent PubMed query, broken down by all TFs (top) and those associated with neurodevelopmental TFs (bottom) (B) Number of candidate papers retrieved from each data resource. Papers associated with neurodevelopmental TFs are highlighted in blue. (C) Pairwise overlap of candidate papers among the different sources shown as fractions of the "target" source (horizontal axis). For example, TRRUST contains 0.48 of the papers recorded in CytReg whereas CytReg contains only 0.05 of the papers in TRRUST. Only values of 0.05 or higher are displayed. External resources are ordered by the number of recorded publications. (D) Summary of associations between TFs and candidate papers. Each point on the left vertical axis is a TF, ordered by the number of candidate papers assigned (TFs with the highest number of candidate papers are at the bottom). Neurodevelopmental TFs are highlighted in blue. Each point on the right vertical axis is a candidate paper, ordered by the number of associated TF (papers with the highest number of candidate papers are at the bottom). Each line denotes a TF-paper association. For example, TBR1 (highlighted) is associated with eight candidate papers (red lines), the PubMed IDs of three papers are printed as examples.

We assessed coverage of TFs among the retrieved set of candidate papers. We found that 90% of all the publications recorded in previous curation databases were covered by the top 316 TFs. Similarly, 90% of all candidate papers queried from PubMed were covered by the top 289

bioRxiv preprint doi: https://doi.org/10.1101/2021.04.11.439248; this version posted April 12, 2021. The copyright holder for this preprint (which was not certified by peer review) is the author/funder, who has granted bioRxiv a license to display the preprint in perpetuity. It is made available under aCC-BY 4.0 International license.

TFs. The set of top TFs in previous curation databases overlaps substantially with the set of top TFs identified in our independent PubMed query (Jaccard Index = 0.52), suggesting shared biases. The overall pattern is shown in Fig 2D. Further, a substantial fraction of TFs (749; 34%) had no candidate papers. Importantly, some key neurodevelopmental TFs appear to have had very limited investigation. For example, TBR1 is a TF recently implicated in Intellectual Disability (ID) and Autism Spectrum Disorder (ASD) (24). Despite this, we were able to identify only eight candidate papers for this gene (Fig 2D), suggesting that TBR1 was not previously popular enough to warrant much attention. We hypothesized that this bias in TF coverage reflects gene popularity differences in general. As expected, we found that the total number of papers per TF in PubMed is highly correlated with the number of candidate papers retrieved (Spearman's correlation = 0.86). As we discuss later, these biases in the literature influence the resulting database of interactions and its interpretation.

Identification of 1,499 experimentally verified TF-target interactions

In total, we recorded 3,601 experiments by examining 1,310 research publications, providing high resolution evidence for 1,499 unique DTRIs involving 251 TFs and 825 targets (Fig 3A, S. Table S3). A small fraction (204; 14%) of all DTRIs were supported by evidence in both humans and mice (Fig 3A). About half (798; 53%) were reported only for mice and the remainder (497; 33%) only for humans. We were able to annotate 39 TFs with 10 or more DTRIs (Fig 3C). Collectively, these top 39 TFs regulate more than half (1018; 68%) of all curated DTRIs. The remaining 481 (32%) DTRIs were distributed across 212 TFs (S. Fig S1). Unsurprisingly given our TF selection criteria, 31 of the top 39 TFs, are associated with neurodevelopment (Fig 3C). Notably, PAX6, a key TF implicated in corticogenesis (25,26) has 63 recorded targets. Further, we identified 12 targets with ten or more recorded TF regulators (S.

bioRxiv preprint doi: https://doi.org/10.1101/2021.04.11.439248; this version posted April 12, 2021. The copyright holder for this preprint (which was not certified by peer review) is the author/funder, who has granted bioRxiv a license to display the preprint in perpetuity. It is made available under aCC-BY 4.0 International license.

193 Fig S2). Eight of these 12 targets are themselves neurodevelopmental TFs including HES1,
194 ASCL1, NEUROG2, MEF2C among others (S. Fig S3). In particular, HES1, a TF known to be
195 involved in the proliferation of neural progenitors (27), has 14 experimentally verified TF
196 regulators.

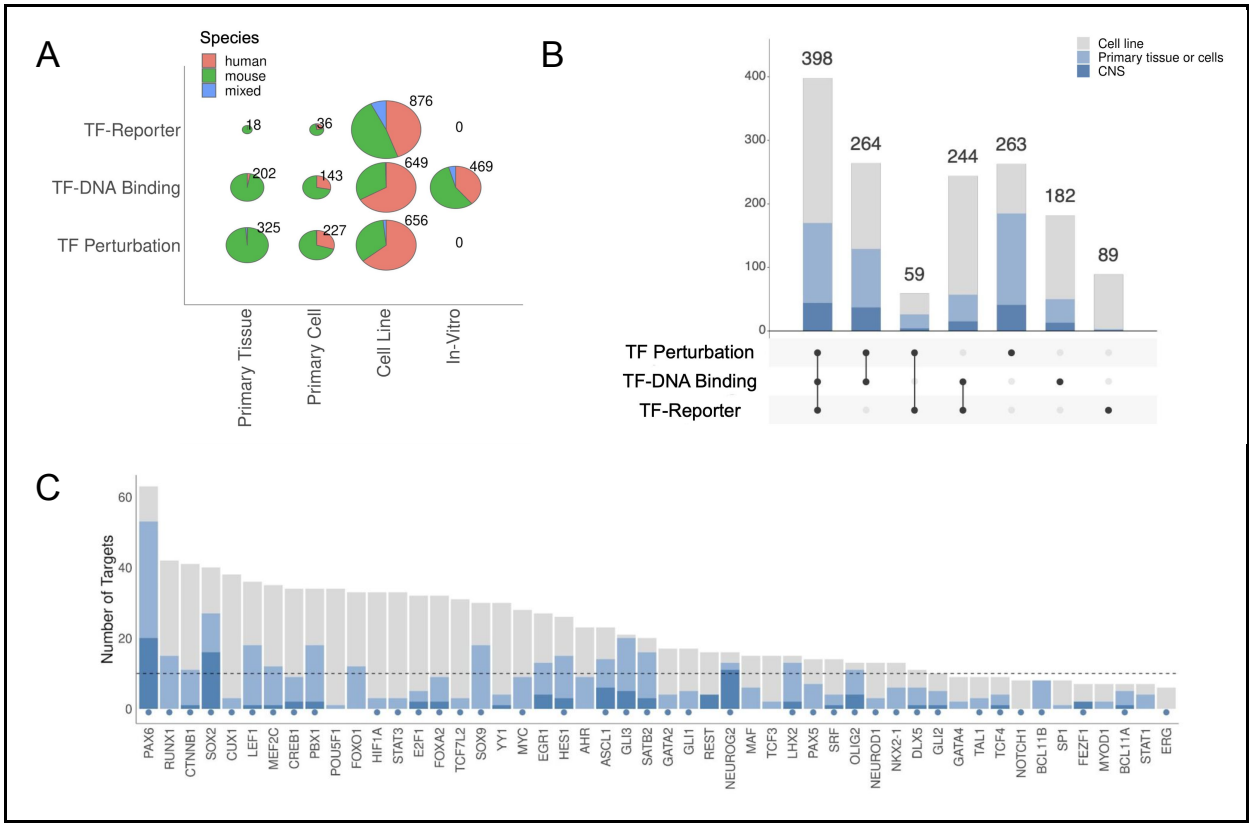

197

198 **Fig 3.** Summary of recorded DTRIs.
199 (A) Breakdown of recorded experiments across experiment types and context types. The “in-vitro” category only
200 includes EMSA experiments for testing TF-DNA binding. (B) Breakdown of DTRIs across different combinations of
201 experiment types. Colors correspond to cellular contexts indicated in the color legend. (C) Number of targets per TF
202 for the top 50 TFs. Color coding is the same as in (B). Neurodevelopmental TFs are indicated by blue circles. There
203 are 39 TFs with more than ten targets (denoted by the horizontal dotted line).

204 Next, we looked at the overall patterns of experimental evidence underlying the recorded
205 DTRIs. TF-DNA binding experiments were most common (1,463), followed by 1,208 TF
206 perturbation and 930 TF-reporter assays (Fig 3A). The majority of all three types of experiments

bioRxiv preprint doi: https://doi.org/10.1101/2021.04.11.439248; this version posted April 12, 2021. The copyright holder for this preprint (which was not certified by peer review) is the author/funder, who has granted bioRxiv a license to display the preprint in perpetuity. It is made available under aCC-BY 4.0 International license.

have been performed using immortalized cell lines (2,181 experiments) rather than primary tissues or cells (951 experiments). This was especially true for reporter assays where close to 95% (876/930) of the experiments were performed using cell lines (Fig 3A). Despite the overall small number of experiments using primary tissue or cells, close to half of all DTRIs (620; 41%) were validated using at least one such experiment. Further, we found that the majority (965; 64%) of DTRIs were supported by two or more types of evidence and 398 (27%) DTRIs were supported by all three (Fig 3B). Of the DTRIs with all three types of evidence, 170 had been tested using primary tissues or cells and 44 had been tested directly in the CNS (Fig 3B).

For each type of experiment, we further explored a number of factors that may influence reliability of the reported DTRI (Table 1). For instance, in TF perturbation assays, there have been reported concerns with artifacts in using overexpression, reviewed in (28). The majority (845; 70%) of TF perturbation experiments recorded were performed by knocking down or knocking out TF expression, although we identified a fraction (363; 30%) of experiments that used overexpression (S. Fig S4, S. Table S5). Further, in TF perturbation experiments that use primary tissues or cells, time-limited modifications may be preferred. Importantly, we found that it is common (373 experiments) to induce a constitutive loss-of-function mutation in the TF and then compare the resulting target gene expression to that of wildtype samples (S. Fig S4). Because the genetic manipulation is present throughout development, the resulting differences may not be entirely attributable to direct regulation by the perturbed TF. Of the 550 TF perturbation experiments performed using primary tissues or cells, 177 (32%) induced the perturbation closer to the time of assay by employing strategies such as Cre-LoxP or RNA interference. For TF-DNA binding experiments, we found that the majority of experiments (994; 68%) used chromatin immunoprecipitation to test for in-vivo binding events in either primary

bioRxiv preprint doi: https://doi.org/10.1101/2021.04.11.439248; this version posted April 12, 2021. The copyright holder for this preprint (which was not certified by peer review) is the author/funder, who has granted bioRxiv a license to display the preprint in perpetuity. It is made available under aCC-BY 4.0 International license.

samples (345 experiments) or immortalized cell lines (649 experiments) (S. Fig S5, S. Table S6). However, EMSAs were also commonly employed to test for in-vitro TF protein-DNA interactions (469 experiments). The reliability of EMSAs might be improved by using the endogenous TF protein, as opposed to using recombinant versions. We found a small number of EMSA experiments (48) that used TF proteins obtained by nuclear extractions directly from primary tissues or cells (S. Figure S5; S. Table S6). Finally, for TF-reporter experiments, we recorded whether mutated versions of the TFBS sequence were assayed to confirm a direct binding mechanism. We found that 407 of the 930 reporter gene assays examined the functional consequence of mutating the corresponding TFBS sequence (S. Fig S6, S. Table S6). Overall, the granularity of our curation highlighted a wide range in the quality and quantity of evidence supporting the reported DTRIs.

Our curation also accounted for tissues and cell types, which we recorded at the highest resolution possible with existing ontologies. This allows subdivision of the data in terms of relevance to particular contexts. In total, 951 (26%) experiments recorded (for 620 DTRIs) were performed using primary tissues or cells. In terms of anatomical systems, among these experiments, the most represented was the CNS, with 243 experiments (155 DTRIs) (S. Fig S7). The set of DTRIs in the CNS is highly enriched for neurodevelopmental TFs (p-value $< 5.6 \times 10^{-9}$, hypergeometric test). Further, a large fraction (181; 74%) of these experiments used embryonic CNS samples, thus providing evidence of activity in the developing CNS (S. Figure S7). For example, ASCL1, FGF19, and SOX2 were reported to regulate targets in the embryonic telencephalon (29), diencephalon (30), and neural stem cells (31), respectively. We also found some DTRIs involving known neurodevelopmental TFs that were assayed only in other tissues, such as a small number of PAX6 targets in pancreatic islets (32,33) and small and large intestine

bioRxiv preprint doi: https://doi.org/10.1101/2021.04.11.439248; this version posted April 12, 2021. The copyright holder for this preprint (which was not certified by peer review) is the author/funder, who has granted bioRxiv a license to display the preprint in perpetuity. It is made available under aCC-BY 4.0 International license.

(34). Over half (2,181; 60%) of all experiments were performed in cell lines, regardless of the experiment type (Fig 3A). Among these, the most popular were kidney derived cell lines (S. Figure S8). As expected, cell line experiments accounted for a larger proportion of human samples compared to primary tissue or cells (Fig 3A). Our detailed information about cellular contexts allows efficient and accurate data subsetting based on user requirements.

Next, we assessed overlaps with other DTRI resources. Since we sourced many candidate papers directly from such earlier curation efforts, a significant amount of overlap is expected. By examining 657 previously curated papers, we managed to extract 809 DTRIs from 467 papers but failed to identify low-throughput experimental evidence in the remaining 190 papers (Fig 4A, S. Table S1). At the level of DTRIs, 40% of our database overlaps with TRRUST while other resources contain up to 8% of our records (S. Fig S9). Limited overlap is common among the other resources as well, with the overwhelming majority of DTRIs having been recorded only in a single database (Fig 4B). This demonstrates the general incomplete coverage of the literature even by the most comprehensive curation efforts to date. Despite being smaller than most other resources (Fig 4C), we still managed to identify 775 DTRIs that were not previously curated in any other database, 541 of which directly involved a neurodevelopmental TF (Fig 4D). Importantly, 449 (58%) of these newly identified interactions were supported by multiple lines of experimental evidence (Fig 4E). Taken together, our curation has expanded the repertoire of annotated DTRIs among the existing DTRI data resources.

bioRxiv preprint doi: https://doi.org/10.1101/2021.04.11.439248; this version posted April 12, 2021. The copyright holder for this preprint (which was not certified by peer review) is the author/funder, who has granted bioRxiv a license to display the preprint in perpetuity. It is made available under aCC-BY 4.0 International license.

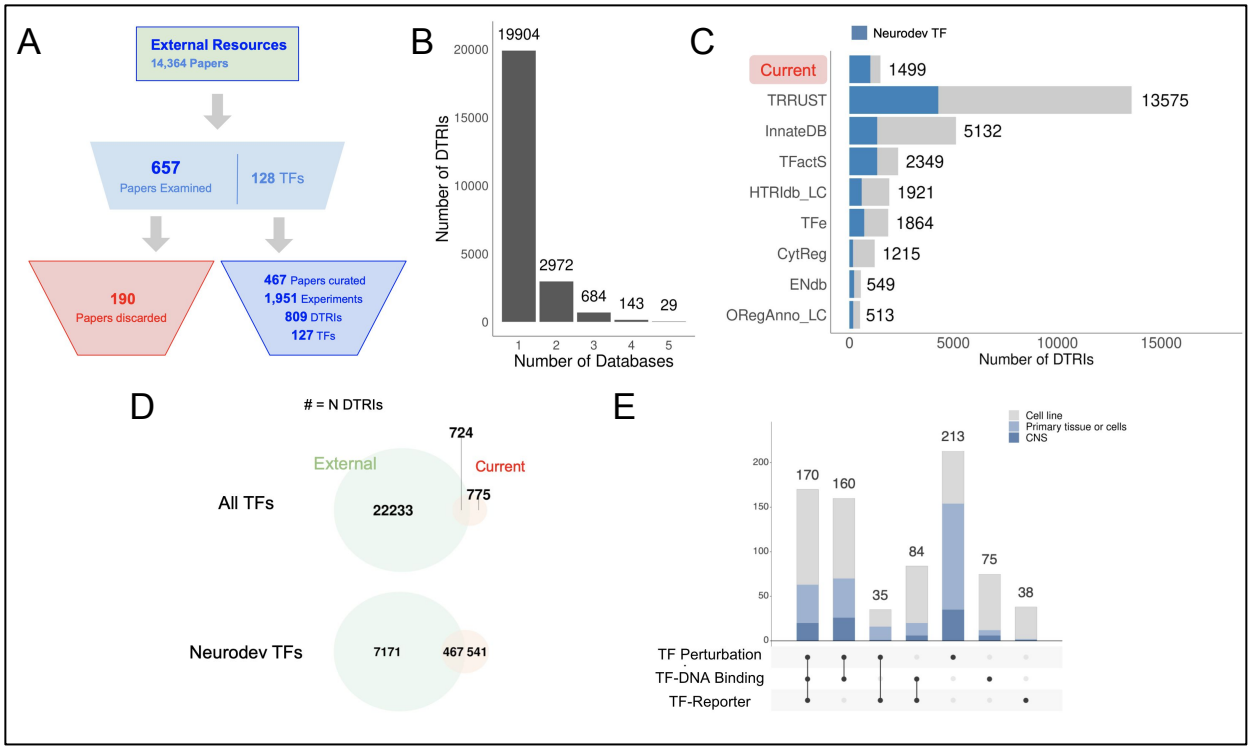

Figure 4. Comparison with external resources. (A) Flow chart of candidate papers obtained from seven external resources. (B) Distribution of DTRIs across the number of resources. Most DTRIs are only recorded in a single database whereas 29 DTRIs are recorded in five databases. No DTRIs have been recorded by more than five databases. (C) Number of DTRIs in each database. DTRIs involving neurodevelopmental TF regulators are highlighted in blue. (D) Venn diagrams showing the overlap between DTRIs recorded in previous curation databases versus the current study, broken down by all TFs (top) and those associated with neurodevelopmental TFs (bottom). (E) Breakdown of DTRIs unique to our curation across different combinations of experiment types. Colors correspond to cellular contexts indicated in the color legend.

Because we curated only a fraction of the literature, it is of interest to estimate the total number of DTRI reports with low-throughput experimental evidence in the remainder. We base our estimate on the observation that of the 1,310 candidate papers that we examined, 63% (828) were found to contain at least one report of DTRI. It follows that approximately >12,000 of the remaining 20,043 candidate papers contain experimental evidence of DTRI. With an average of 1.9 DTRIs reported by any single publication (S. Fig S10), there would be >22,000 DTRIs remaining in the literature, in addition to the 1,499 DTRIs already curated. Limiting to the 8,730

bioRxiv preprint doi: https://doi.org/10.1101/2021.04.11.439248; this version posted April 12, 2021. The copyright holder for this preprint (which was not certified by peer review) is the author/funder, who has granted bioRxiv a license to display the preprint in perpetuity. It is made available under aCC-BY 4.0 International license.

candidate papers annotated with neurodevelopmental TFs, there would be >10,000 more DTRIs. As noted above, we found that under a third (398/1,499) of all recorded DTRIs were supported by all three types of experimental evidence. Further, about half (170) of these high confidence DTRIs had been tested in primary tissues or cells, and of these, 44 were tested directly in the CNS. Assuming the set of candidate papers is representative, there would be around >6,000 (0.3*22,000) more DTRIs that are supported by all three types of evidence and >600 (0.03*22,000) of these would have been tested using primary CNS tissues or cells. By extension, we estimate our curation of 44 DTRIs with high confidence verification of activity in the CNS captures up to 7% of all such DTRIs reported in the literature. Taken together, we estimate that there remain many thousands of additional high-confidence DTRIs in the published literature which could be the subject of future curation efforts.

Network properties reflect potential research biases

Given the literature biases in coverage of TFs (Fig 2D), we suspected that similar biases may exist in the selection of regulatory targets. Specifically, researchers may be more likely to choose to investigate interactions between genes that are suspected to be related. If this is true, the manually curated network should be more connected than expected if the targets were chosen randomly. To test this, we integrated all DTRIs in our database to construct a directed network consisting of 955 nodes and 1,499 edges (Fig 1D). We measured network connectivity in three ways. First, we counted the number of valid gene-to-gene paths in the network. Briefly, for every gene in the network, we counted the number of other genes that are within reach via at least one continuous path. The total count was then obtained by summing across all genes. Because the edges are directed and the network consists of multiple components, not every gene is reachable from every other gene in the network. In total, we observed more than 77,000 gene-to-gene paths

bioRxiv preprint doi: https://doi.org/10.1101/2021.04.11.439248; this version posted April 12, 2021. The copyright holder for this preprint (which was not certified by peer review) is the author/funder, who has granted bioRxiv a license to display the preprint in perpetuity. It is made available under aCC-BY 4.0 International license.

311 in the curated network, which is significantly higher than the mean of 55,411 paths among a null
312 constructed from random networks ($p < 0.01$; see Methods). This indicates a high degree of
313 global connectivity within the network. Next, we counted the number of cliques with three or
314 more nodes, ignoring directionality. We found 215 cliques in the curated network, which is
315 higher than a mean of 140 cliques among the random networks (p-value < 0.01), demonstrating a
316 large number of locally interconnected modules. Finally, we observed only four independent
317 components in the curated network whereas a typical random network had 26 components (p-
318 value < 0.01), implying that even peripheral genes with low node degrees remain connected to
319 the rest of the network. Taken together, the manually curated network is highly interconnected,
320 even after controlling for biases in TF coverage. This strongly suggests substantial biases in the
321 selection of targets by investigators, as observed for TF selection.

322 Continuing our investigation of biases in the data, we hypothesized that TSS proximal
323 cREs would be enriched among the reported DTRIs since distal elements are likely more
324 difficult to identify. We define proximal regulatory elements to be either promoters or regulatory
325 elements that fall within 3 kb of the target TSS, as indicated by the original publication. We
326 found that most (595 of 663 DTRIs where the TFBS position was annotated) of the reported
327 DTRIs involve proximal cREs and only 68 DTRIs have been annotated with distal regulatory
328 sites (S. Fig S11, S. Fig S12). Distal sites include the well-documented interaction between
329 SOX2 and SHH where the corresponding enhancer is 5 kb downstream of the TSS (Favaro et al.,
330 2009). Such cases are, by far, the minority in our curation. In addition to TFBS proximity, we
331 also annotated whether a regulatory interaction is activating or repressive, referred to as the
332 mode of regulation (Table 1). We found that about less than a third (313/1,317) of the DTRIs are
333 repressive (S. Fig S11). It is less clear whether this trend reflects underlying biological trends or

bioRxiv preprint doi: https://doi.org/10.1101/2021.04.11.439248; this version posted April 12, 2021. The copyright holder for this preprint (which was not certified by peer review) is the author/funder, who has granted bioRxiv a license to display the preprint in perpetuity. It is made available under aCC-BY 4.0 International license.

another form of investigator bias in the selection of interactions to study. Notably, several repressive DTRIs involve TFs that are generally characterized as repressors including HES1, GLI3, and REST (S. Fig S13). In particular, HES1 was annotated to repress 16 of its 26 targets (among the 23 targets where the mode of regulation was reported). The majority of other TFs have been found to upregulate the expression of the majority of their target genes. For example, RUNX1 represents a typical example that activates expression of 80% (30/37) of its recorded targets. A small number (23) of DTRIs have been reported to be both activating and repressive in different experiments. Overall, of all 557 DTRIs where both the mode of regulation and the cRE positions are known, 411 (74%) involve activation of proximal cREs and only five (<1%) are repression of a distal cRE.

Comparison with a high throughput TF perturbation screen in the embryonic mouse forebrain

One application of our curated DTRI resource is to benchmark high-throughput screens. To demonstrate this use case, we analyzed a previously published TF perturbation screen for Pax6 (Fig 5A). In this study, the authors sought to identify Pax6 targets in the embryonic mouse forebrain by examining genome wide differential expression between wildtype and Pax6 mutant mice using microarrays (35). We assessed enrichment of our curated PAX6/Pax6 targets in this dataset (this includes targets validated in either humans or mice). We found that 22 of all 56 curated PAX6/Pax6 targets were differentially expressed at a false discovery rate (FDR) of 0.1 (p-value < 4.4×10^{-6}, hypergeometric test; similar results were obtained with a threshold-free comparison (S. Fig S14)). Among these include several known neurodevelopmental genes such as ASCL1, SOX2, and NEUROG2 (Fig 5A). We conclude there is significant correspondence between the curated targets and the high-throughput differential expression screen.

bioRxiv preprint doi: https://doi.org/10.1101/2021.04.11.439248; this version posted April 12, 2021. The copyright holder for this preprint (which was not certified by peer review) is the author/funder, who has granted bioRxiv a license to display the preprint in perpetuity. It is made available under aCC-BY 4.0 International license.

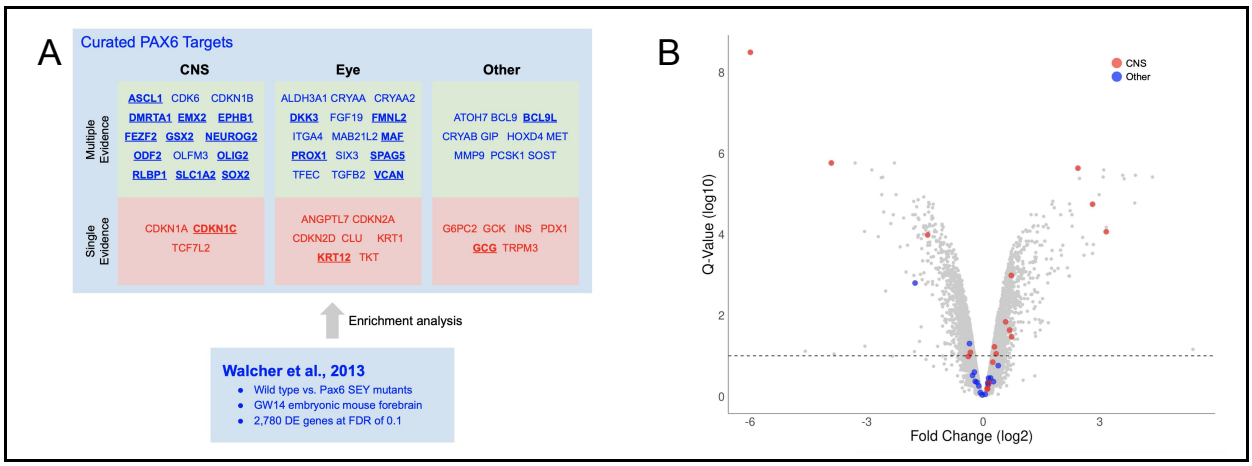

357

358 **Figure 5.** Comparison with a high-throughput Pax6 perturbation screen. (A) Summarized result of the comparative
359 analysis. Curated PAX6/Pax6 targets are organized by tissue and number of types of experimental evidence. Genes
360 differentially expressed at FDR of 0.1 are bolded and underlined. (B) Volcano plot of differential expressions between
361 wildtype and Pax6-Sey mouse embryonic forebrains. Curated PAX6/pax6 targets are highlighted with tissue
362 specificity as depicted in the color legend. Fold change ($\log_2$) is displayed in x-axis. Multiple test corrected q-values
363 (Benjamini-Hochberg Procedure) are plotted on the y-axis on a log10 scale. Dotted line indicates 0.1 FDR for
364 reference. Curated CNS targets are highly overrepresented in the differentially expression profile (p-value < 1.4×10^{-7},
365 hypergeometric test) whereas no overrepresentation was detected for the targets in the "Other" category (p-value <
366 0.8, hypergeometric test).
367

368 In the analysis above, we ignored context, but it is plausible that low-throughput
369 experiments performed in the same tissue as Walcher et al. (2013) would yield even higher
370 correspondence. To test for this, we divided the PAX6/Pax6 targets into three tissue types: the
371 CNS, the eye, and "other", with the latter containing mostly DTRIs validated in cell lines. Since
372 the differential expression profile was generated in the embryonic mouse forebrain, we
373 hypothesized that the targets supported by low-throughput CNS evidence would be most highly
374 enriched. We found that this is indeed the case. Thirteen of 18 CNS targets were differentially
375 expressed at an FDR of 0.1 (p-value < 8.5×10^{-9}, hypergeometric test) (Fig 5B). This is nearly a
376 twofold improvement over the set of all curated PAX6/Pax6 targets. Again, this observation was

bioRxiv preprint doi: https://doi.org/10.1101/2021.04.11.439248; this version posted April 12, 2021. The copyright holder for this preprint (which was not certified by peer review) is the author/funder, who has granted bioRxiv a license to display the preprint in perpetuity. It is made available under aCC-BY 4.0 International license.

corroborated by an additional threshold-free analysis (S. Fig S15). Further, we confirmed that the increase in the level enrichment for CNS targets over the set of all PAX6/Pax6 targets was statistically significant by using a resampling strategy to estimate the 95th percentile confidence intervals of the enrichment values (S. Fig S16). The level of enrichment for targets validated in the eye is approximately the same as the set of all targets (7 of 22 targets were differentially expressed at FDR of 0.1; p-value < $1.5x10^{-2}$, hypergeometric test). Finally, we did not observe enrichment for the set of targets in the "other" category (2 of 16 targets were differentially expressed at FDR of 0.1; p-value < 0.47, hypergeometric test) (Fig 5B, S. Fig S15, S. Fig S16). Similar to cellular contexts, we also found significant difference in the level of enrichment between the curated targets with single vs. multiple types of recorded experiments (S. Fig S16, S. Fig S17). These results provide a proof-of-principle for using our curation resource to evaluate high-throughput screens.

Discussion

The elucidation of the genetic circuits underpinning neurodevelopmental disorders has been a major challenge. While there has been progress in the development of TRN reconstruction methods using high-throughput data, it is reasonable to ask how much has already been captured in the lengthy history of low-throughput experiments, and to make maximal use of this information. Because low-throughput methods appear to be considered reliable (they are often used to validate high-throughput methods), especially when there are multiple lines of evidence, having a high-quality assembly of such data would be beneficial. In our survey of previous efforts to produce such resource, we identified the lack of detail about the amount and type of low-throughput evidence to be a major gap. To this end, we undertook a systematic and detailed effort to inspect the published literature for support of DTRIs at the individual

bioRxiv preprint doi: https://doi.org/10.1101/2021.04.11.439248; this version posted April 12, 2021. The copyright holder for this preprint (which was not certified by peer review) is the author/funder, who has granted bioRxiv a license to display the preprint in perpetuity. It is made available under aCC-BY 4.0 International license.

experiment level. We show that this approach improves interpretability of a curated DTRI data resource. Here, we release the result of our curation for use by the wider research community.

The significance of having experiment level details is emphasized by our observation of the variation in confidence levels across the reported DTRIs in the published literature. A summary analysis of our database has revealed that only a fraction of all reported DTRIs is supported by all three types of experimental evidence. Similarly, most experiments were carried out using cell lines that may not recapitulate in-vivo activity. Even within a single type of experiment, we observed important differences in approach that may further impact reliability. This pattern of varied confidence among the reported DTRIs was largely unreported in previous curation efforts. The practical utility of our curation is further demonstrated by the comparison with the high-throughput Pax6 perturbation screen. The significantly higher levels of enrichment among the targets verified directly in the CNS and by multiple evidence types further confirms that our curation approach is appropriate for compiling bona fide DTRIs in the low-throughput literature.

Among all the external resources reviewed, CytReg (16) and ENdb (13) were the only studies with explicit consideration of different types of experimental evidence. In CytReg, the authors classified experiments into functional or binding assays, abstracting away other details that would further enhance interpretability. In ENdb, the authors focused on the annotation of enhancers, with limited curation of details on specific TF-target interactions. TFe, on the other hand, took a more implicit approach to account for reliability (21). Instead of using a systematic curation approach, TFe relied on annotations of TF-target interactions by community experts, who in turn evaluate the merits of individual studies on an ad hoc basis. A recent report provided evidence to support the quality of the DTRIs recorded in TFe (36). However, the fractured

bioRxiv preprint doi: https://doi.org/10.1101/2021.04.11.439248; this version posted April 12, 2021. The copyright holder for this preprint (which was not certified by peer review) is the author/funder, who has granted bioRxiv a license to display the preprint in perpetuity. It is made available under aCC-BY 4.0 International license.

423 curation process makes this approach have questionable scalability. TRRUST is the largest
424 literature-based resource to date (14,15). Using a semi-automated text mining approach,
425 TRRUST recorded pairs of interacting genes from publication abstracts, purposely overlooking
426 the underlying experimental details. The remaining databases including OReganno (17–19),
427 HTRIdb (20), TFactS (22), and InnateDB (23) rely solely on TF binding experiments to indicate
428 direct regulation. Finally, with the exception of InnateDB and ENdb, none of the previous
429 curation efforts recorded information about the cellular context.

430 There are still a number of limitations to our work. In general, manual curation can have
431 errors. In order to minimize mistakes, we established and strictly followed a formal curation
432 protocol. In particular, we introduced controlled vocabularies for all recorded attributes to
433 simplify the curation process. All records were checked twice, and any conflicts were resolved
434 by the first author. Next, incomplete retrieval of candidate papers is a potential concern. While
435 we strived to find as many papers as possible using both previous curation resources and
436 independent PubMed queries, it is plausible that we have missed some candidate papers given
437 our selection of and reliance on the MeSH search terms. Nonetheless, the pronounced popularity
438 biases we report are unlikely to be an artifact of our search strategy. Further, since we aimed to
439 curate only a handful of DTRIs for a small set of TFs of interest, an incomplete pool of candidate
440 papers was not a major issue. However, for a more comprehensive curation effort with the goal
441 of increasing coverage of less popular TFs, it is possible that a future study may benefit from
442 using more elaborate text mining approaches for retrieving candidate papers.

443 In order to establish a direct binding mechanism for regulatory interactions with the
444 highest possible confidence, the effect of modifying cREs in their endogenous chromosomal loci
445 should be considered. Emerging studies are using CRISPR-KRAB and related approaches to

bioRxiv preprint doi: https://doi.org/10.1101/2021.04.11.439248; this version posted April 12, 2021. The copyright holder for this preprint (which was not certified by peer review) is the author/funder, who has granted bioRxiv a license to display the preprint in perpetuity. It is made available under aCC-BY 4.0 International license.

perform this analysis; recent examples include (37,38). However, such studies are few, and therefore have not been included in our curation protocol. Instead, we focused only on the three most commonly reported types of experimental evidence. In the future, it may be possible to integrate such data types in order to improve reliability beyond current standards.

The lack of a negative set may limit the utility of this resource for validation. For example, in the PAX6/Pax6 analysis we could only assess sensitivity of the high-throughput perturbation study with respect to our database, not specificity. This is because our attempts to find negative examples was largely unsuccessful. During curation, we took note of any TF perturbation or TF-reporter experiments that yielded negative results in the papers that we examined. We only found 11 such cases (S. Table S11). There are two possible reasons for this. First, our search for candidate papers may be biased against experiments with negative results. If this is the case, it may be possible to improve the search strategy to identify more relevant papers. However, it is more plausible that the literature itself is depleted of negative reports, due to "the file-drawer problem" (39). Future work should attempt to identify negative examples by performing further experimentation or by developing alternative heuristics.

It is also important to emphasize that the network we obtained here cannot and should not be used for large scale biological inference, because the structure of the network is strongly influenced by research biases and the relationship with the true regulatory network is very uncertain. The highly skewed TF coverage among the candidate papers, coupled with the correlation between the number of candidate papers and gene popularity implies that researchers generally choose to study DTRIs involving TFs of previously known significance. Conversely, some genes, such as TBR1, are functionally important but lack experimental characterization, perhaps due to their more recently discovered functional roles. This general research bias,

bioRxiv preprint doi: https://doi.org/10.1101/2021.04.11.439248; this version posted April 12, 2021. The copyright holder for this preprint (which was not certified by peer review) is the author/funder, who has granted bioRxiv a license to display the preprint in perpetuity. It is made available under aCC-BY 4.0 International license.

combined with biases of our curation, has obvious impacts on the resulting network structure. Previous work by our group has documented the impact of bias towards well studied, multifunctional genes in other types of network analyses (40). Our observation of the high internode connectivity in the curated network demonstrates the presence of DTRI biases beyond gene popularity. Likewise, it is unclear whether the skewed representation of DTRIs involving activation of proximal cREs is the result of research bias or a real biological pattern. As such, we caution against interpretations based on the properties of the manually curated network.

We curated what we estimate to be a substantial, but still small, fraction of the relevant literature. Fortunately, our curation protocol can be scaled up to produce a considerably larger collection of high confidence DTRIs. According to our estimates, our current curation has captured less than ten percent of all experimentally verified DTRIs reported in the published literature. The bulk of our curation was performed in four months by two full time curators. Given this experience, we estimate an exhaustive curation effort could be completed by a team of ten curators in approximately 12 months. Importantly, we predict that about a third of all reported DTRIs would be supported by all three types of experimental evidence. However, we take note of the scarcity of specific DTRIs in particular contexts. In particular, we found less than 5% of all recorded DTRIs to have reliably demonstrated activity specifically in the CNS. While we postulate that a manual curation approach is required to establish a high confidence DTRI catalogue for training and validating high-throughput predictions, the aforementioned biases and scarcity of low-throughput experiments will prevent the use of manually curated networks directly for analysis. To elucidate the architecture of gene regulation underpinning neurodevelopment and disease, it is imperative to develop effective means for accurately

bioRxiv preprint doi: https://doi.org/10.1101/2021.04.11.439248; this version posted April 12, 2021. The copyright holder for this preprint (which was not certified by peer review) is the author/funder, who has granted bioRxiv a license to display the preprint in perpetuity. It is made available under aCC-BY 4.0 International license.

predicting DTRIs based on high-throughput data. This curation effort supports progress towards this end.

Methods

All data analyses and visualizations were performed using R and R-Studio (2015). Data plots were made using ggplot2 (Wickham, 2011). For data manipulation, we used Tidyverse (Wickham et al., 2019).

Obtaining records from external resources

We obtained records from eight external databases: ENdb, TRRUST, CytReg, OReganno, HTRIdb, TFe, TFactS, and InnateDB. We downloaded the ENdb records from http://www.licpathway.net/ENdb/ on Sept. 14th, 2020. Records from the remaining databases were downloaded between Dec. 9 and Dec. 16, 2019. We obtained the CytReg records from the supplementary data of the original publication. For TRRUST, we downloaded both the human and mouse data tables directly from https://www.grnpedia.org/trrust/. An additional column was added to preserve the species annotation before joining the two tables. The most recent version of the records in ORegAnno were obtained from http://www.oreganno.org/. Here, we retained only records with valid Entrez or Ensembl ID, and PubMed ID annotations. In addition, records annotated as miRNA regulation or those resulting from high-throughput screens were excluded. We downloaded InnateDB records from https://www.innatedb.com/ and filtered for records reporting protein-DNA interactions. The TFe records were retrieved from the now deprecated web API, http://cisreg.cmmt.ubc.ca/cgi-bin/tfe. Species information was inferred from the TF gene symbols recorded in TFe. The TFactS records were downloaded from http://www.tfacts.org/. A union set was derived by merging both signed and signless data tables

bioRxiv preprint doi: https://doi.org/10.1101/2021.04.11.439248; this version posted April 12, 2021. The copyright holder for this preprint (which was not certified by peer review) is the author/funder, who has granted bioRxiv a license to display the preprint in perpetuity. It is made available under aCC-BY 4.0 International license.

513 in TFactS. Finally, for HTRIdb, we downloaded the data from http://www.lbbc.ibb.unesp.br/htri.
514 Here, we filtered for literature curated records with valid PubMed ID annotations.

515 From each database we retained records of one-to-one regulator-target interactions with
516 annotations in either human or mouse. We indexed genes using Entrez IDs. In cases where only
517 the gene symbols were available, we mapped the symbols to Entrez IDs, first by using the
518 official HGNC or MGI symbols and then by gene aliases. With the exception of ENdb, which
519 was published after we completed curation, the retrieved set of publications was used as a source
520 of candidate papers for curation in the present study (S. Table S1). Each publication was
521 assigned to one or more TFs based on the recorded DTRIs. Additionally, we also retained
522 species information and modes of regulation where available. For all analysis and reporting, we
523 matched all TF and target genes to human orthologs using NCBI HomoloGene (Maglott et al.,
524 2005, Mancarci and French, 2019: https://cran.r-
525 project.org/web/packages/homologene/index.html). When there are no human orthologs, the
526 mouse Entrez gene is used directly. Independent regulatory interactions were defined as unique
527 combinations of the human TF and target genes.

528 **Identification of neurodevelopmental TFs**

529 We define TFs to be either the genes annotated with least one regulatory target in any of
530 the previous resources or those identified as TFs by Lambert et al. (41). Collectively, this TF set
531 consists of 2,235 genes. Given our particular focus in this study on neurodevelopment, we
532 further designated 438 TFs as neurodevelopmental TFs based Gene Ontology annotations, and
533 disease association records from SFARI (S. Table S2) (42,43). We downloaded the list of genes
534 annotated with the central nervous system development GO term (GO:0007417) or any of its

bioRxiv preprint doi: https://doi.org/10.1101/2021.04.11.439248; this version posted April 12, 2021. The copyright holder for this preprint (which was not certified by peer review) is the author/funder, who has granted bioRxiv a license to display the preprint in perpetuity. It is made available under aCC-BY 4.0 International license.

descendent terms for both human and mouse from AmiGO (http://amigo.geneontology.org/). Next, we downloaded the list of genes associated with neurodevelopmental disorders from the SFARI database (https://gene.sfari.org/). The list of TFs is provided in S. Table S2. Finally, we manually prioritized these TFs for curation based on the annotated association with neurodevelopment and the number of candidate papers retrieved.

Obtaining candidate publications for curation

In addition to the candidate papers derived from the external resources, we also performed an independent PubMed query for each TF (refer to the previous section for the operational definition of a TF). We took advantage of the E-Utilities API provided by NCBI to perform searches programmatically (44). We selected six MeSH terms that indicate experimental evidence for: "Regulatory Sequences, Nucleic Acid", "Transcription, Genetic", "Intracellular Signaling Peptides and Proteins", "Gene Expression Regulation", "Chromatin Immunoprecipitation", and "Electrophoretic Mobility Shift Assay". The set of the selected search terms were appended to the gene symbol of each TF to form an independent search query to obtain the corresponding set of candidate papers. To approximate gene popularity of TFs, we performed another round of PubMed query for each TF using only the gene symbol without the MeSH terms.

Experiment-centric curation of DTRIs

For each paper that we examined, we recorded all low-throughput experimental evidence of DTRIs. Specifically, we look for three types of experiments: TF perturbation, TF-DNA binding, and TF-reporter assays. As such, each experiment constitutes an independent record in the database and is assigned a unique identifier (S. Table S3). Gene identifiers were translated

bioRxiv preprint doi: https://doi.org/10.1101/2021.04.11.439248; this version posted April 12, 2021. The copyright holder for this preprint (which was not certified by peer review) is the author/funder, who has granted bioRxiv a license to display the preprint in perpetuity. It is made available under aCC-BY 4.0 International license.

into Entrez IDs at the time of recording. Species information was recorded separately for the TF and the target genes. The context type may be cell lines, or primary tissue or cells. In the case of EMSA experiments, the context types are designated to be in-vitro. In addition to the context type, we further annotated each experiment with a specific ontology term in order to retain the highest context resolution possible. We used terms from the UBERON ontology (45) for primary tissue, the CL ontology (46) for primary cells, and the CLO ontology (47) for cell lines. Where the appropriate ontology term could not be found in the aforementioned ontologies, we additionally used terms from the BTO (48) and the EFO (49) ontologies. When all else fails, we directly recorded the name provided in the original publication. Age was also recorded as a separate attribute for experiments that used primary tissues or cells. Where available, we also recorded the direction of regulation as well as whether the reported regulatory element is proximal or distal to the TSS of the target gene. Proximal elements were defined to be either promoters or cREs within 3 kb upstream or downstream of the TSS. Table 1 contains the full list of recorded attributes and the corresponding descriptions.

For each type of experiment, we selected a number of details. For TF perturbation experiments, we recorded whether the TF was overexpressed, down regulated, or knocked out. We also recorded whether the perturbation was dynamically induced before the time of assay or constitutively modified at the beginning of life. For TF-DNA binding experiments, we recorded both ChIP-assay and EMSA experiments. For EMSA, we further annotated the source of the TF protein. Finally, for reporter assays, we recorded whether mutations were introduced to the cRE sequence for comparison.

Network analysis

bioRxiv preprint doi: https://doi.org/10.1101/2021.04.11.439248; this version posted April 12, 2021. The copyright holder for this preprint (which was not certified by peer review) is the author/funder, who has granted bioRxiv a license to display the preprint in perpetuity. It is made available under aCC-BY 4.0 International license.

To assess the connectivity of the manually curated network, we used the iGraph package in R (50). First, we constructed a directed network consisting of all curated DTRIs. Three metrics were computed to measure internode connectivity: the number of valid gene-to-gene paths, the number of cliques with three or more nodes, and the number of independent components. To assess statistical significance, we constructed 1000 network permutations by randomly swapping all edges while preserving both in and out degrees of all nodes. This set of random networks were then used to generate empirical null distributions for each of the three metrics. One-tailed p-values were computed by obtaining the fraction of random values larger or smaller than the observed values.

Comparison with the high-throughput Pax6 perturbation screen

We selected PAX6/Pax6, the TF with the highest number of recorded targets, for assessing correspondence with a high-throughput screen. We obtained the genome wide expression data generated by previous study (35) along with the metadata from Gemma (51). This dataset was selected for its relevance to brain development. We then performed a differential expression analysis between the wild type and the Pax6-Sey samples using limma (52). This resulted in a list of genes with p-values representing significance of differential expression upon Pax6 knockout. For hit list analyses, we used a cut-off FDR of 0.1. We used the ranking of nominal p-values for AUROC analyses. The Entrez IDs for the mouse genes were mapped to human orthologs using HomoloGene so that the results could be compared with the current curation.

Next, we took all 56 curated targets for PAX6/Pax6 that were present in the microarray dataset and sliced it according to cellular context and quality of evidence. To retrieve targets with

bioRxiv preprint doi: https://doi.org/10.1101/2021.04.11.439248; this version posted April 12, 2021. The copyright holder for this preprint (which was not certified by peer review) is the author/funder, who has granted bioRxiv a license to display the preprint in perpetuity. It is made available under aCC-BY 4.0 International license.

demonstrated activity in the CNS, we retrieved all interactions for PAX6/Pax6 where there is at least one experiment annotated with the CNS ontology term (UBERON:0001017) or any of its descendent terms. Similarly, we searched for all targets annotated with the eye term (UBERON:0000970). Targets with evidence in both the CNS and the eye were placed only in the CNS category so that the categories are mutually exclusive. The remaining targets were classified as "other". To subset by quality of evidence, we binned all PAX6/Pax6 targets into those with multiple types of experiments vs. only a single type of experiment.

Each of these target subsets were then tested for enrichment in the high-throughput differential expression screen. Enrichment was tested in two ways. First, a hit list of 2,780 differentially expressed genes were generated using an FDR threshold. Overrepresentation of the curated targets in this list was tested by using the hypergeometric distribution, yielding a p-value for each set of curated targets. Next, we generated a ranking of differentially expressed genes using nominal p-values and used the AUROC method to test enrichment for each set of curated targets towards the top of this ranking. AUROCs were computed by using the Mann-Whitney U Test. To test for significant differences among the AUROCs for the different target subsets, we estimated the variance of the AUROC for each subset by bootstrapping 1000 random samples for each set of curated targets. Significant differences were determined by assessing the overlaps among 95th percentile confidence intervals.

Acknowledgement

We thank Dr. Shamsuddin Bhuiyan for providing advice on setting up the initial curation protocol. We thank Nathaniel Lim for providing the formatted ontology hierarchy files for tissue

bioRxiv preprint doi: https://doi.org/10.1101/2021.04.11.439248; this version posted April 12, 2021. The copyright holder for this preprint (which was not certified by peer review) is the author/funder, who has granted bioRxiv a license to display the preprint in perpetuity. It is made available under aCC-BY 4.0 International license.

and cell type analyses. We thank Dr. Shamsuddin Bhuiyan, Dr. Marjan Farahbod, and Dr. Sanja Rogic for advice on writing and providing feedback on an early draft.

Data Availability

All relevant data are within the manuscript and its Supporting Information files. The code for all data analyses and figures generation are available on GitHub (https://github.com/PavlidisLab/dtri-curation). An additional copy of the data has been deposited in Scholars Portal Dataverse (https://doi.org/10.5683/SP2/XLLWRL).

Financial Disclosure

This work was supported by National Institutes of Health grant MH111099 (https://www.nih.gov/) and Natural Sciences and Engineering Research Council of Canada grant RGPIN-2016-05991 (https://www.nserc-crsng.gc.ca/), both held by PP. EC and AM were supported, in part, by the NSERC-CREATE program in High-Dimensional Bioinformatics at UBC (https://www.grad.ubc.ca/prospective-students/research/nserc-create-programs). EC additionally received funding from the UBC ECOSCOPE training program (http://ecoscope.ubc.ca/) and AM received the IMH Marshall Scholarship from the UBC Department of Psychiatry (https://psychiatry.ubc.ca/). AS was supported, in part, by an NSERC undergraduate student award (https://www.nserc-crsng.gc.ca/). The funders had no role in study design, data collection and analysis, decision to publish, or preparation of the manuscript.

List of Figures

Figure 1. Summary of curation

Figure 2. Overall landscape of the candidate papers retrieved

bioRxiv preprint doi: https://doi.org/10.1101/2021.04.11.439248; this version posted April 12, 2021. The copyright holder for this preprint (which was not certified by peer review) is the author/funder, who has granted bioRxiv a license to display the preprint in perpetuity. It is made available under aCC-BY 4.0 International license.

643 **Figure 3.** Summary of recorded DTRIs

644 **Figure 4.** Comparison with external resources

645 **Figure 5.** Comparison with a high-throughput Pax6 perturbation screen

646 **Supplementary Figure S1.** Distribution of TFs by the number of recorded targets

647 **Supplementary Figure S2.** Distribution of targets by the number of recorded TF

648 **Supplementary Figure S3.** Number of TFs per target for the top 50 TFs

649 **Supplementary Figure S4.** Detailed summary of TF perturbation experiments

650 **Supplementary Figure S5.** Detailed summary of TF-DNA binding experiments

651 **Supplementary Figure S6.** Detailed summary of TF-reporter experiments

652 **Supplementary Figure S7.** Breakdown of experiments performed using primary tissues or cells
653 across anatomical systems

654 **Supplementary Figure S8.** Breakdown of experiments performed using cell lines across broad
655 cell type categories

656 **Supplementary Figure S9.** Pairwise overlap of DTRIs among the different data resources

657 **Supplementary Figure S10.** Distribution of papers by the number of DTRIs reported

658 **Supplementary Figure S11.** Breakdown of DTRIs by mode of regulation and TFBS position

659 **Supplementary Figure S12.** TFBS Position of DTRIs per TF for the top 50 TFs

660 **Supplementary Figure S13.** Mode of regulation of DTRIs per TF for the top 50 TFs

661 **Supplementary Figure S14.** Enrichment of all curated PAX6/Pax6 targets among differentially
662 expressed genes in the Pax6 TF perturbation dataset

663 **Supplementary Figure S15.** Enrichment of curated PAX6/Pax6 targets among differentially
664 expressed genes in the Pax6 TF perturbation dataset by tissue types

bioRxiv preprint doi: https://doi.org/10.1101/2021.04.11.439248; this version posted April 12, 2021. The copyright holder for this preprint (which was not certified by peer review) is the author/funder, who has granted bioRxiv a license to display the preprint in perpetuity. It is made available under aCC-BY 4.0 International license.

Supplementary Figure S16. AUROC values for the different categories of curated PAX6/Pax6 targets

Supplementary Figure S17. Enrichment of curated PAX6/Pax6 targets among differentially expressed genes in the Pax6 TF perturbation dataset, by single or multiple types of experimental evidence

List of Tables

Table 1. Experimental details recorded during curation

Supplementary Table S1. List of candidate papers

Supplementary Table S2. List of TFs

Supplementary Table S3. Curated records at the experiment level

Supplementary Table S4. Curated records summarized at the DTRI level

Supplementary Table S5. TF Perturbation experiment details

Supplementary Table S6. TF-DNA Binding experiment details

Supplementary Table S7. TF-reporter experiment details

Supplementary Table S8. All DTRI records including those curated in external databases

Supplementary Table S9. Records obtained from external databases

Supplementary Table S10. List of differentially expressed genes following Pax6 perturbation

Supplementary Table S11. Experiments with negative results

References

1. Pearl JR, Colantuoni C, Bergey DE, Funk CC, Shannon P, Basu B, et al. Genome-Scale Transcriptional Regulatory Network Models of Psychiatric and Neurodegenerative Disorders. Cell Syst. 2019 Feb;8(2):122-135.e7.

bioRxiv preprint doi: https://doi.org/10.1101/2021.04.11.439248; this version posted April 12, 2021. The copyright holder for this preprint (which was not certified by peer review) is the author/funder, who has granted bioRxiv a license to display the preprint in perpetuity. It is made available under aCC-BY 4.0 International license.

687 2. Miraldi ER, Pokrovskii M, Watters A, Castro DM, Veaux ND, Hall JA, et al. Leveraging
688 chromatin accessibility for transcriptional regulatory network inference in T Helper 17
689 Cells. Genome Res. 2019 Jan 3;29(3):449–63.

690 3. Ament SA, Pearl JR, Cantle JP, Bragg RM, Skene PJ, Coffey SR, et al. Transcriptional
691 regulatory networks underlying gene expression changes in Huntington's disease. Mol Syst
692 Biol. 2018 Mar 1;14(3):e7435.

693 4. Sonawane AR, Platig J, Fagny M, Chen C-Y, Paulson JN, Lopes-Ramos CM, et al.
694 Understanding Tissue-Specific Gene Regulation. Cell Rep. 2017 Oct 24;21(4):1077–88.

695 5. Satterstrom FK, Kosmicki JA, Wang J, Breen MS, Rubeis SD, An J-Y, et al. Large-Scale
696 Exome Sequencing Study Implicates Both Developmental and Functional Changes in the
697 Neurobiology of Autism. Cell [Internet]. 2020 Jan 23 [cited 2020 Jan 23];0(0). Available
698 from: https://www.cell.com/cell/abstract/S0092-8674(19)31398-4

699 6. De Rubeis S, He X, Goldberg AP, Poultney CS, Samocha K, Ercument Cicek A, et al.
700 Synaptic, transcriptional and chromatin genes disrupted in autism. Nature [Internet]. 2014
701 Oct 29 [cited 2014 Oct 29];advance online publication. Available from:
702 http://www.nature.com/nature/journal/vaop/ncurrent/full/nature13772.html?WT.ec_id=NA
703 TURE-20141030

704 7. O'Roak BJ, Deriziotis P, Lee C, Vives L, Schwartz JJ, Girirajan S, et al. Exome sequencing
705 in sporadic autism spectrum disorders identifies severe de novo mutations. Nat Genet. 2011
706 Jun;43(6):585–9.

707 8. Williams SM, An JY, Edson J, Watts M, Murigneux V, Whitehouse AJO, et al. An
708 integrative analysis of non-coding regulatory DNA variations associated with autism
709 spectrum disorder. Mol Psychiatry [Internet]. 2018 Apr 27 [cited 2018 May 15]; Available
710 from: http://www.nature.com/articles/s41380-018-0049-x

711 9. Turner TN, Eichler EE. The Role of De Novo Noncoding Regulatory Mutations in
712 Neurodevelopmental Disorders. Trends Neurosci [Internet]. 2018 Dec 15 [cited 2019 Jan
713 17]; Available from: http://www.sciencedirect.com/science/article/pii/S0166223618302960

714 10. Takata A, Ionita-Laza I, Gogos JA, Xu B, Karayiorgou M. De Novo Synonymous
715 Mutations in Regulatory Elements Contribute to the Genetic Etiology of Autism and
716 Schizophrenia. Neuron. 2016 Mar 2;89(5):940–7.

717 11. Sun J, Rockowitz S, Xie Q, Ashery-Padan R, Zheng D, Cvekl A. Identification of in vivo
718 DNA-binding mechanisms of Pax6 and reconstruction of Pax6-dependent gene regulatory
719 networks during forebrain and lens development. Nucleic Acids Res. 2015 Aug
720 18;43(14):6827–46.

721 12. Scardigli R, Bäumer N, Gruss P, Guillemot F, Roux IL. Direct and concentration-dependent
722 regulation of the proneural gene Neurogenin2 by Pax6. Development. 2003 Jul
723 15;130(14):3269–81.

bioRxiv preprint doi: https://doi.org/10.1101/2021.04.11.439248; this version posted April 12, 2021. The copyright holder for this preprint (which was not certified by peer review) is the author/funder, who has granted bioRxiv a license to display the preprint in perpetuity. It is made available under aCC-BY 4.0 International license.

13. Bai X, Shi S, Ai B, Jiang Y, Liu Y, Han X, et al. ENdb: a manually curated database of experimentally supported enhancers for human and mouse. Nucleic Acids Res. 2020 Jan 8;48(D1):D51–7.

14. Han H, Cho J-W, Lee S, Yun A, Kim H, Bae D, et al. TRRUST v2: an expanded reference database of human and mouse transcriptional regulatory interactions. Nucleic Acids Res. 2018 Jan 4;46(D1):D380–6.

15. Han H, Shim H, Shin D, Shim JE, Ko Y, Shin J, et al. TRRUST: a reference database of human transcriptional regulatory interactions. Sci Rep. 2015 Jun 12;5(1):11432.

16. Carrasco Pro S, Dafonte Imedio A, Santoso CS, Gan KA, Sewell JA, Martinez M, et al. Global landscape of mouse and human cytokine transcriptional regulation. Nucleic Acids Res. 2018 Oct 12;46(18):9321–37.

17. Lesurf R, Cotto KC, Wang G, Griffith M, Kasaian K, Jones SJM, et al. ORegAnno 3.0: a community-driven resource for curated regulatory annotation. Nucleic Acids Res. 2016 Jan 4;44(D1):D126-132.

18. Griffith OL, Montgomery SB, Bernier B, Chu B, Kasaian K, Aerts S, et al. ORegAnno: an open-access community-driven resource for regulatory annotation. Nucleic Acids Res. 2008 Jan 1;36(suppl_1):D107–13.

19. Montgomery SB, Griffith OL, Sleumer MC, Bergman CM, Bilenky M, Pleasance ED, et al. ORegAnno: an open access database and curation system for literature-derived promoters, transcription factor binding sites and regulatory variation. Bioinformatics. 2006 Mar 1;22(5):637–40.

20. Bovolenta LA, Acencio ML, Lemke N. HTRIdb: an open-access database for experimentally verified human transcriptional regulation interactions. BMC Genomics. 2012;13(1):405.

21. Yusuf D, Butland SL, Swanson MI, Bolotin E, Ticoll A, Cheung WA, et al. The Transcription Factor Encyclopedia. Genome Biol. 2012 Mar 29;13(3):R24.

22. Essaghir A, Toffalini F, Knoops L, Kallin A, van Helden J, Demoulin J-B. Transcription factor regulation can be accurately predicted from the presence of target gene signatures in microarray gene expression data. Nucleic Acids Res. 2010 Jun;38(11):e120.

23. Lynn DJ, Winsor GL, Chan C, Richard N, Laird MR, Barsky A, et al. InnateDB: facilitating systems-level analyses of the mammalian innate immune response. Mol Syst Biol [Internet]. 2008 Sep 2 [cited 2013 Jun 5];4(1). Available from: http://www.nature.com/msb/journal/v4/n1/full/msb200855.html

24. Nambot S, Faivre L, Mirzaa G, Thevenon J, Bruel A-L, Mosca-Boidron A-L, et al. De novo TBR1 variants cause a neurocognitive phenotype with ID and autistic traits: report of 25 new individuals and review of the literature. Eur J Hum Genet. 2020 Jun;28(6):770–82.

bioRxiv preprint doi: https://doi.org/10.1101/2021.04.11.439248; this version posted April 12, 2021. The copyright holder for this preprint (which was not certified by peer review) is the author/funder, who has granted bioRxiv a license to display the preprint in perpetuity. It is made available under aCC-BY 4.0 International license.

25. Georgala PA, Carr CB, Price DJ. The role of Pax6 in forebrain development. Dev Neurobiol. 2011;71(8):690–709.

26. Talamillo A, Quinn JC, Collinson JM, Caric D, Price DJ, West JD, et al. Pax6 regulates regional development and neuronal migration in the cerebral cortex. Dev Biol. 2003 Mar 1;255(1):151–63.

27. Baek JH, Hatakeyama J, Sakamoto S, Ohtsuka T, Kageyama R. Persistent and high levels of Hes1 expression regulate boundary formation in the developing central nervous system. Development. 2006 Jul 1;133(13):2467–76.

28. Gibson TJ, Seiler M, Veitia RA. The transience of transient overexpression [Internet]. Nature Methods. 2013 [cited 2018 Apr 23]. Available from: https://www.nature.com/articles/nmeth.2534

29. Castro DS, Skowronska-Krawczyk D, Armant O, Donaldson IJ, Parras C, Hunt C, et al. Proneural bHLH and Brn Proteins Coregulate a Neurogenic Program through Cooperative Binding to a Conserved DNA Motif. Dev Cell. 2006 Dec 1;11(6):831–44.

30. Martinez-Ferre A, Lloret-Quesada C, Prakash N, Wurst W, Rubenstein JLR, Martinez S. Fgf15 regulates thalamic development by controlling the expression of proneural genes. Brain Struct Funct. 2016 Jul 1;221(6):3095–109.

31. Engelen E, Akinci U, Bryne JC, Hou J, Gontan C, Moen M, et al. Sox2 cooperates with Chd7 to regulate genes that are mutated in human syndromes. Nat Genet. 2011 Jun;43(6):607–11.

32. Raum JC, Hunter CS, Artner I, Henderson E, Guo M, Elghazi L, et al. Islet β-Cell-Specific MafA Transcription Requires the 5′-Flanking Conserved Region 3 Control Domain. Mol Cell Biol. 2010 Sep 1;30(17):4234–44.

33. Wen JH, Chen YY, Song SJ, Ding J, Gao Y, Hu QK, et al. Paired box 6 (PAX6) regulates glucose metabolism via proinsulin processing mediated by prohormone convertase 1/3 (PC1/3). Diabetologia. 2009 Mar 1;52(3):504–13.

34. Hill ME, Asa SL, Drucker DJ. Essential requirement for Pax 6 in control of enteroendocrine proglucagon gene transcription. Mol Endocrinol. 1999;13(9):1474–86.

35. Walcher T, Xie Q, Sun J, Irmler M, Beckers J, Öztürk T, et al. Functional dissection of the paired domain of Pax6 reveals molecular mechanisms of coordinating neurogenesis and proliferation. Development. 2013 Mar 1;140(5):1123–36.

36. Garcia-Alonso L, Holland CH, Ibrahim MM, Turei D, Saez-Rodriguez J. Benchmark and integration of resources for the estimation of human transcription factor activities. Genome Res. 2019 Aug;29(8):1363–75.

bioRxiv preprint doi: https://doi.org/10.1101/2021.04.11.439248; this version posted April 12, 2021. The copyright holder for this preprint (which was not certified by peer review) is the author/funder, who has granted bioRxiv a license to display the preprint in perpetuity. It is made available under aCC-BY 4.0 International license.

794 37. Gasperini M, Hill AJ, McFaline-Figueroa JL, Martin B, Kim S, Zhang MD, et al. A
795 Genome-wide Framework for Mapping Gene Regulation via Cellular Genetic Screens. Cell.
796 2019 Jan 10;176(1):377-390.e19.

797 38. Fulco CP, Nasser J, Jones TR, Munson G, Bergman DT, Subramanian V, et al. Activity-by-
798 contact model of enhancer-promoter regulation from thousands of CRISPR perturbations.
799 Nat Genet. 2019;51(12):1664–9.

800 39. Kennedy D. The old file-drawer problem. Science. 2004 Jul 23;305(5683):451.

801 40. Gillis J, Pavlidis P. The impact of multifunctional genes on "guilt by association" analysis.
802 PloS One. 2011;6(2):e17258.

803 41. Lambert SA, Jolma A, Campitelli LF, Das PK, Yin Y, Albu M, et al. The Human
804 Transcription Factors. Cell. 2018 Feb 8;172(4):650–65.

805 42. Abrahams BS, Arking DE, Campbell DB, Mefford HC, Morrow EM, Weiss LA, et al.
806 SFARI Gene 2.0: a community-driven knowledgebase for the autism spectrum disorders
807 (ASDs). Mol Autism. 2013 Oct 3;4(1):36.

808 43. Gene Ontology Consortium. The Gene Ontology (GO) database and informatics resource.
809 Nucleic Acids Res. 2004 Jan 1;32(suppl_1):D258–61.

810 44. NCBI Resource Coordinators. Database Resources of the National Center for
811 Biotechnology Information. Nucleic Acids Res. 2017 Jan 4;45(D1):D12–7.

812 45. Mungall CJ, Torniai C, Gkoutos GV, Lewis SE, Haendel MA. Uberon, an integrative multi-
813 species anatomy ontology. Genome Biol. 2012 Jan 31;13(1):R5.

814 46. Diehl AD, Meehan TF, Bradford YM, Brush MH, Dahdul WM, Dougall DS, et al. The Cell
815 Ontology 2016: enhanced content, modularization, and ontology interoperability. J Biomed
816 Semant. 2016 Jul 4;7(1):44.

817 47. Sarntivijai S, Lin Y, Xiang Z, Meehan TF, Diehl AD, Vempati UD, et al. CLO: The cell
818 line ontology. J Biomed Semant. 2014 Aug 13;5(1):37.

819 48. Gremse M, Chang A, Schomburg I, Grote A, Scheer M, Ebeling C, et al. The BRENDA
820 Tissue Ontology (BTO): the first all-integrating ontology of all organisms for enzyme
821 sources. Nucleic Acids Res. 2011 Jan 1;39(suppl_1):D507–13.

822 49. Malone J, Holloway E, Adamusiak T, Kapushesky M, Zheng J, Kolesnikov N, et al.
823 Modeling sample variables with an Experimental Factor Ontology. Bioinformatics. 2010
824 Apr 15;26(8):1112–8.

825 50. Csardi G, Nepusz T. The igraph software package for complex network research.
826 InterJournal Complex Syst. 2006;1695(5):1–9.

bioRxiv preprint doi: https://doi.org/10.1101/2021.04.11.439248; this version posted April 12, 2021. The copyright holder for this preprint (which was not certified by peer review) is the author/funder, who has granted bioRxiv a license to display the preprint in perpetuity. It is made available under aCC-BY 4.0 International license.

827 51. Zoubarev A, Hamer KM, Keshav KD, McCarthy EL, Santos JRC, Van Rossum T, et al.
828 Gemma: a resource for the reuse, sharing and meta-analysis of expression profiling data.
829 Bioinforma Oxf Engl. 2012 Sep 1;28(17):2272–3.

830 52. Smyth G. Limma: linear models for microarray data. Gentleman RCarey VDudoit SIrizarry
831 RHuber W Bioinformatics and computational biology solutions using R and Bioconductor.
832 New York: Springer; 2005.

833

834

835

836

837

838

839

840

bioRxiv preprint doi: https://doi.org/10.1101/2021.04.11.439248; this version posted April 12, 2021. The copyright holder for this preprint (which was not certified by peer review) is the author/funder, who has granted bioRxiv a license to display the preprint in perpetuity. It is made available under aCC-BY 4.0 International license.

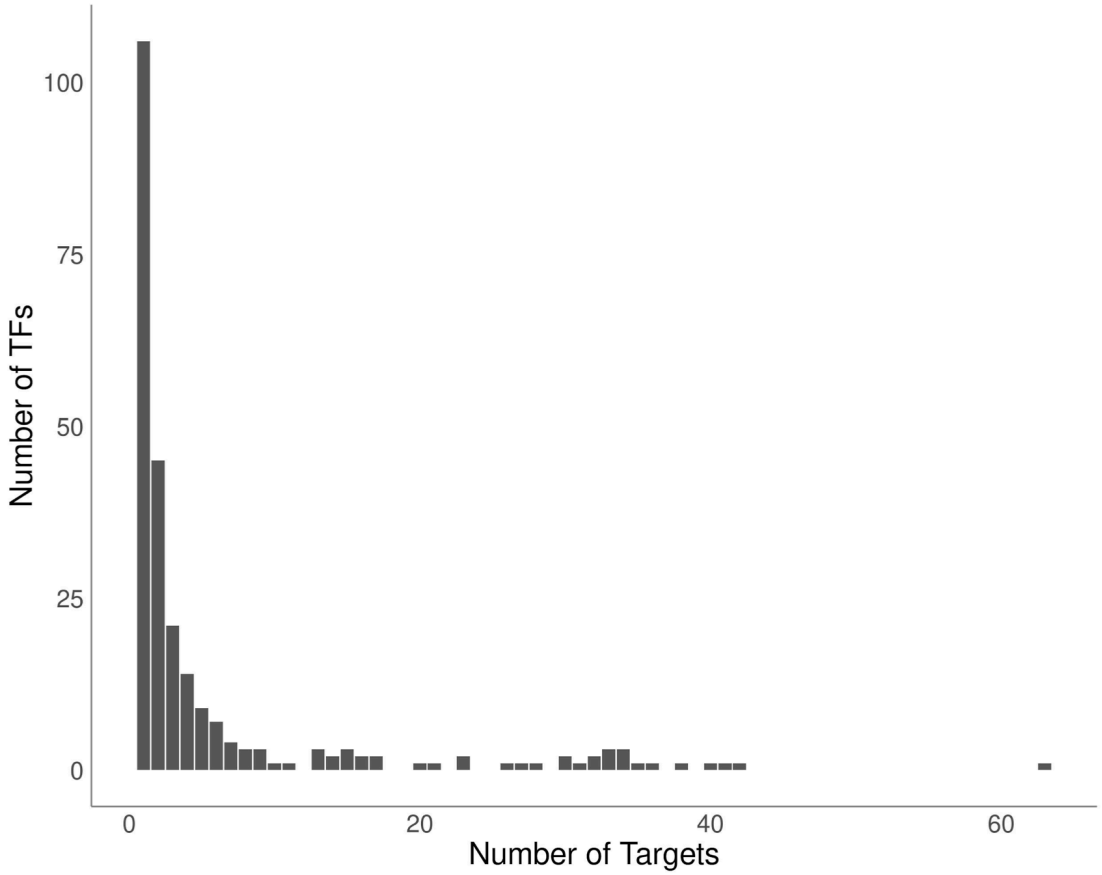

841

842 **Supplementary Figure S1**. Distribution of TFs by the number of targets.

843 Only TFs with at least one curated target are plotted. Most (212/251) TFs have less than ten

844 targets recorded.

845

846

847

848

849

850

bioRxiv preprint doi: https://doi.org/10.1101/2021.04.11.439248; this version posted April 12, 2021. The copyright holder for this preprint (which was not certified by peer review) is the author/funder, who has granted bioRxiv a license to display the preprint in perpetuity. It is made available under aCC-BY 4.0 International license.

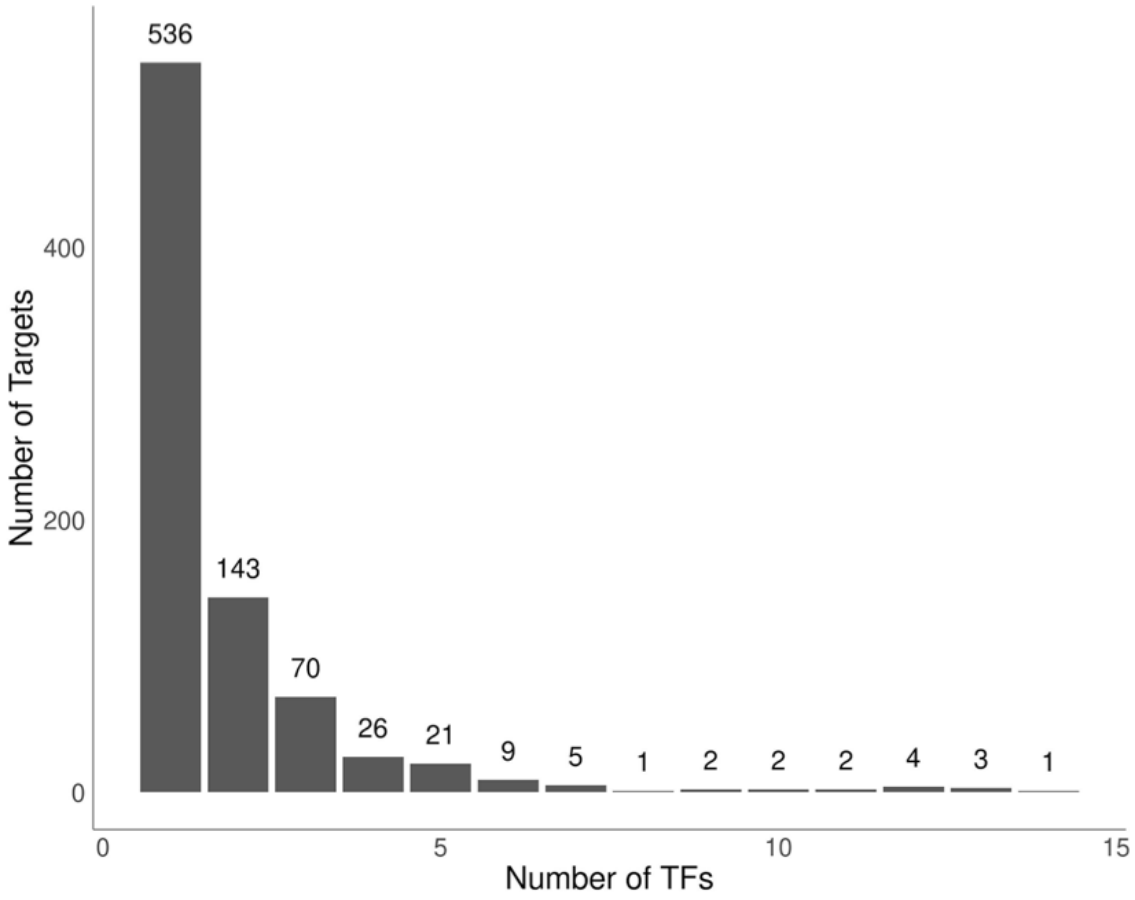

Supplementary Figure S2. Distribution of targets by the number of recorded TF regulators. Only targets with at least one recorded TF regulator are included.

bioRxiv preprint doi: https://doi.org/10.1101/2021.04.11.439248; this version posted April 12, 2021. The copyright holder for this preprint (which was not certified by peer review) is the author/funder, who has granted bioRxiv a license to display the preprint in perpetuity. It is made available under aCC-BY 4.0 International license.

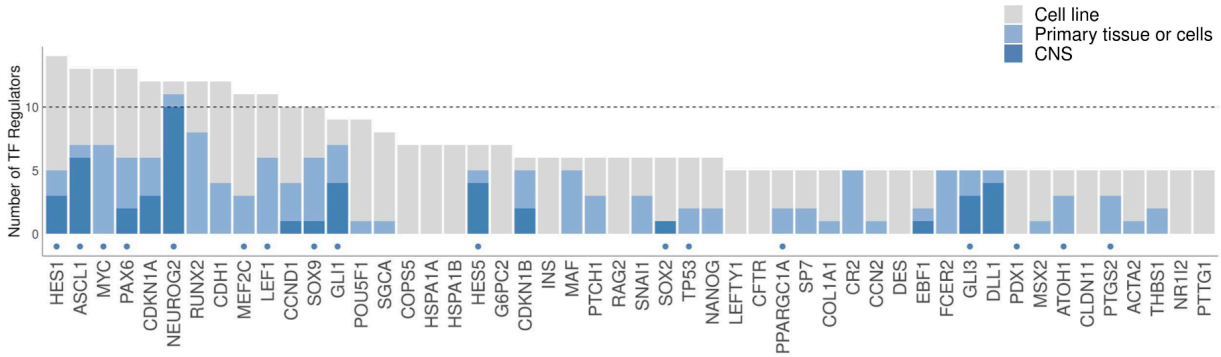

862

863 **Supplementary Figure S3.** Number of TF regulators per target for the top 50 target genes.

864 Target genes that are also neurodevelopmental TFs are indicated by blue dots. Bar colors

865 correspond to cellular contexts indicated in the color legend. There are eight targets with more

866 than 10 recorded TF regulators (denoted by the horizontal dotted line).

867

868

869

870

871

872

bioRxiv preprint doi: https://doi.org/10.1101/2021.04.11.439248; this version posted April 12, 2021. The copyright holder for this preprint (which was not certified by peer review) is the author/funder, who has granted bioRxiv a license to display the preprint in perpetuity. It is made available under aCC-BY 4.0 International license.

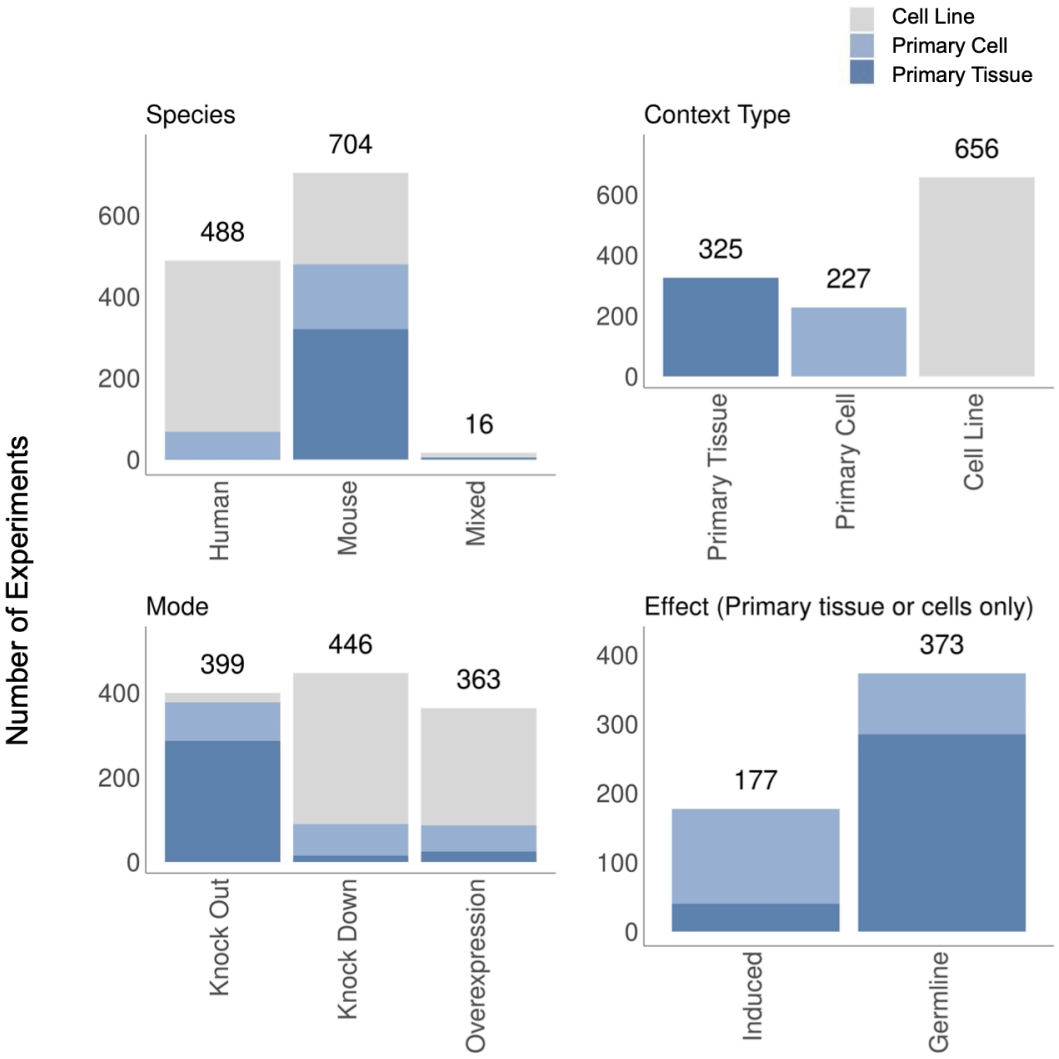

873

874 **Supplementary Figure S4.** Details of TF perturbation experiments.

875 Colors correspond to cellular contexts as indicated in the legend. Top left: Breakdown of

876 experiments by species. The “mixed” column refers to experiments where the TF and the target

877 genes originated from different species, which is possible in TF overexpression experiments.

878 Top right: Breakdown of experiments by context type. Bottom left: Breakdown of experiments

879 by the mode of TF perturbation. “Knock Out” refers perturbations at the genetic level including

880 naturally occurring mutations. Further breakdown into heterozygous or homozygous knock

bioRxiv preprint doi: https://doi.org/10.1101/2021.04.11.439248; this version posted April 12, 2021. The copyright holder for this preprint (which was not certified by peer review) is the author/funder, who has granted bioRxiv a license to display the preprint in perpetuity. It is made available under aCC-BY 4.0 International license.

881 outs are provided in Supplementary Table S5. “Knock Down” refers to transcript level
882 perturbation by RNA interference. Bottom right: Breakdown of experiments by the effect of TF
883 perturbation in primary tissues or cells. “Constitutive” perturbations are present throughout
884 development versus “induced” perturbations are triggered closer to the time of assay.
885
886
887
888
889
890
891
892

bioRxiv preprint doi: https://doi.org/10.1101/2021.04.11.439248; this version posted April 12, 2021. The copyright holder for this preprint (which was not certified by peer review) is the author/funder, who has granted bioRxiv a license to display the preprint in perpetuity. It is made available under aCC-BY 4.0 International license.

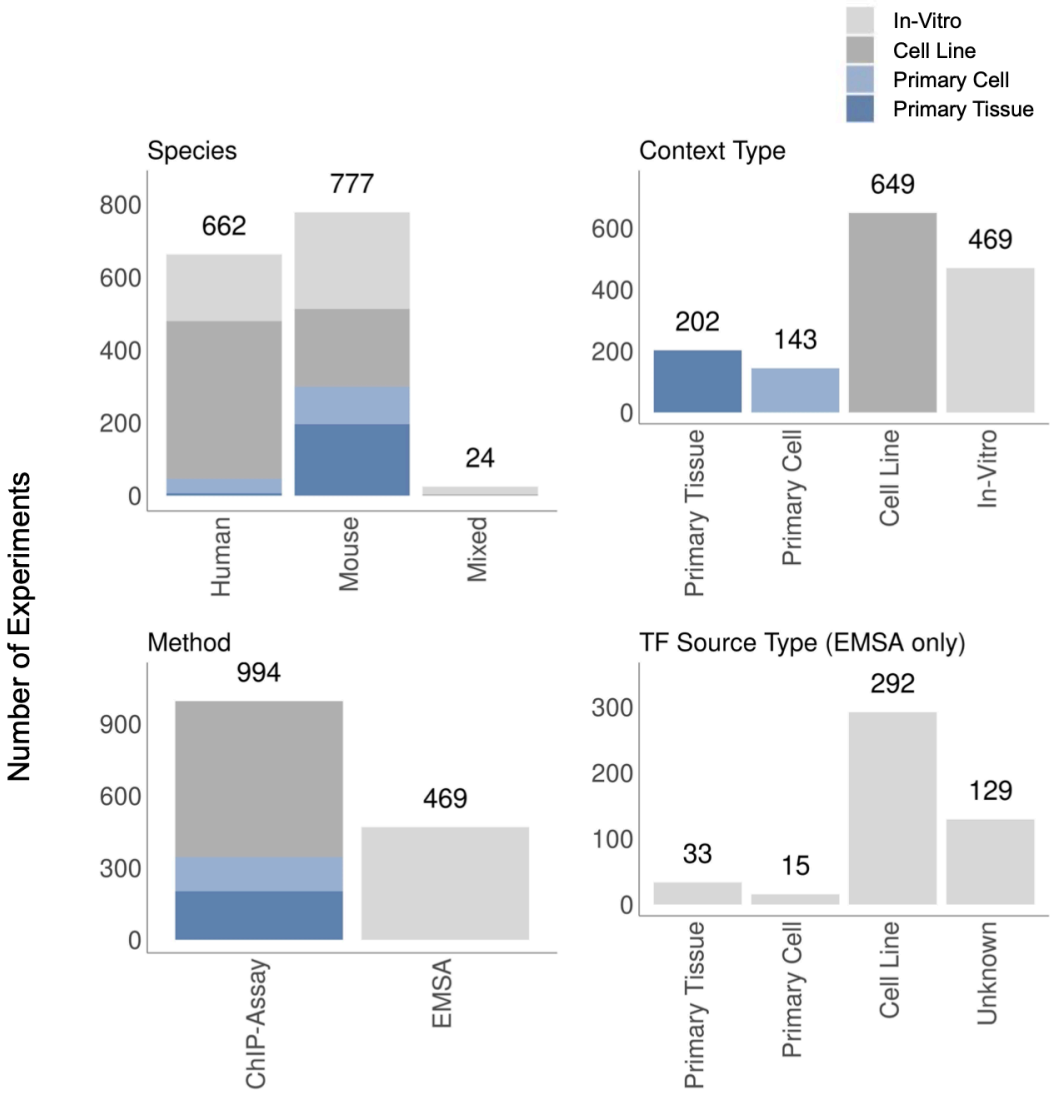

Supplementary Figure S5. Details of TF-DNA binding experiments.

Colors correspond to cellular contexts as indicated in the color legend. Top left: Breakdown of experiments by species. The "mixed" column refers to experiments where the TF and the target genes originated from different species, which is possible in EMSA experiments. Top right: Breakdown of experiments by context type. All EMSA experiments were classified as "in-vitro" for context type. Bottom left: Breakdown of experiments by method. Bottom right: Breakdown of experiments by source of the TF protein in EMSA experiments. Forty-eight EMSA

bioRxiv preprint doi: https://doi.org/10.1101/2021.04.11.439248; this version posted April 12, 2021. The copyright holder for this preprint (which was not certified by peer review) is the author/funder, who has granted bioRxiv a license to display the preprint in perpetuity. It is made available under aCC-BY 4.0 International license.

901 experiments used endogenous TF proteins sourced from primary tissues or cells. In most cases

902 (292), TF proteins were sourced from cell lines following TF transfection.

903

904

905

906

907

908

bioRxiv preprint doi: https://doi.org/10.1101/2021.04.11.439248; this version posted April 12, 2021. The copyright holder for this preprint (which was not certified by peer review) is the author/funder, who has granted bioRxiv a license to display the preprint in perpetuity. It is made available under aCC-BY 4.0 International license.

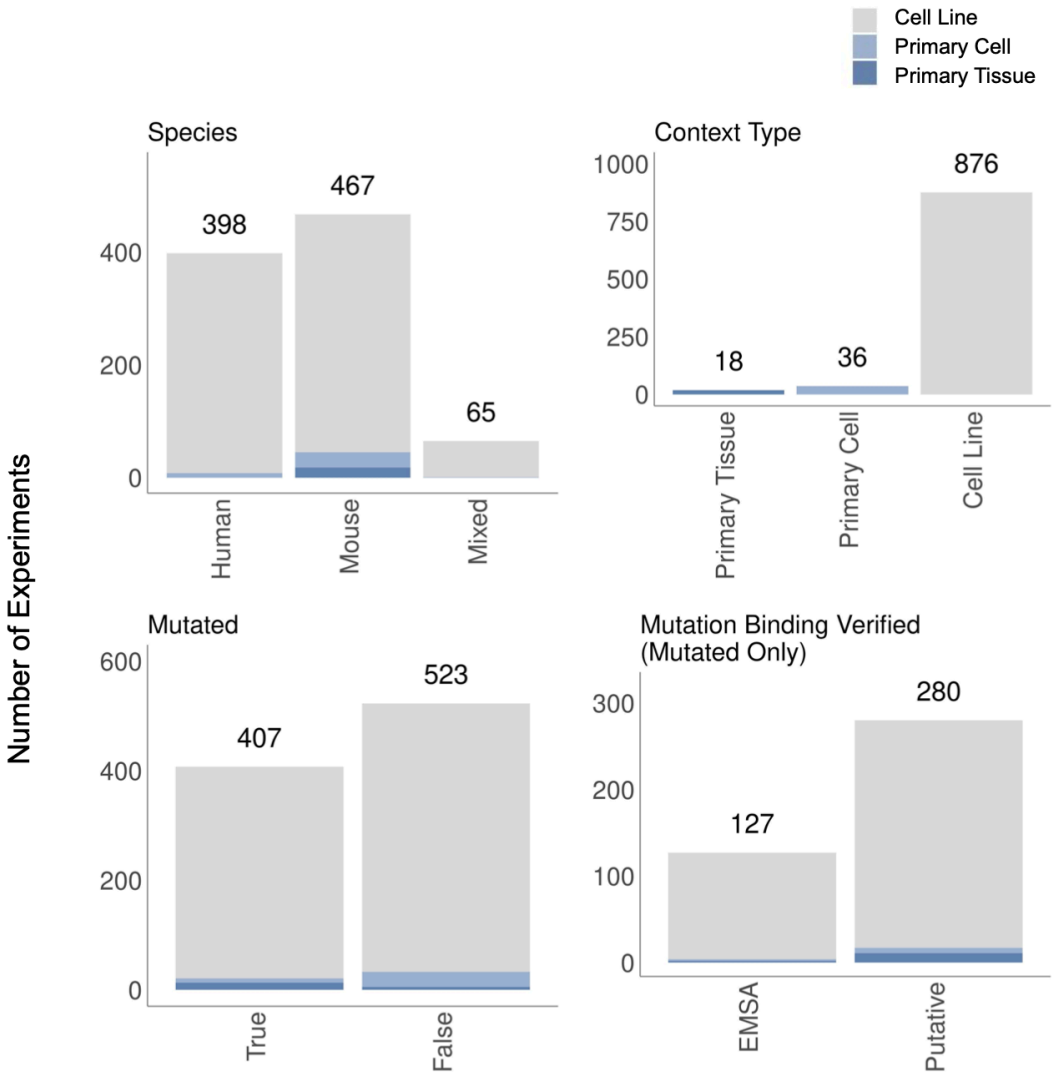

Supplementary Figure S6. Details of TF-reporter experiments.

Colors correspond to cellular contexts as indicated in the color legend. Top left: Breakdown of experiments by species. The "mixed" column refers to experiments where the TF and the target genes originated from different species. Top right: Breakdown of experiments by context type. Few TF-reporter experiments were performed using primary tissues or cells. Bottom left: Breakdown of TF-reporter experiments that did or did not investigate the effect of mutating the

bioRxiv preprint doi: https://doi.org/10.1101/2021.04.11.439248; this version posted April 12, 2021. The copyright holder for this preprint (which was not certified by peer review) is the author/funder, who has granted bioRxiv a license to display the preprint in perpetuity. It is made available under aCC-BY 4.0 International license.

916 corresponding cRE sequence. Bottom right: Breakdown of whether the effect of the mutation
917 on the TF-DNA interaction was confirmed experimentally by EMSA.
918
919
920
921
922
923
924
925
926
927
928

bioRxiv preprint doi: https://doi.org/10.1101/2021.04.11.439248; this version posted April 12, 2021. The copyright holder for this preprint (which was not certified by peer review) is the author/funder, who has granted bioRxiv a license to display the preprint in perpetuity. It is made available under aCC-BY 4.0 International license.

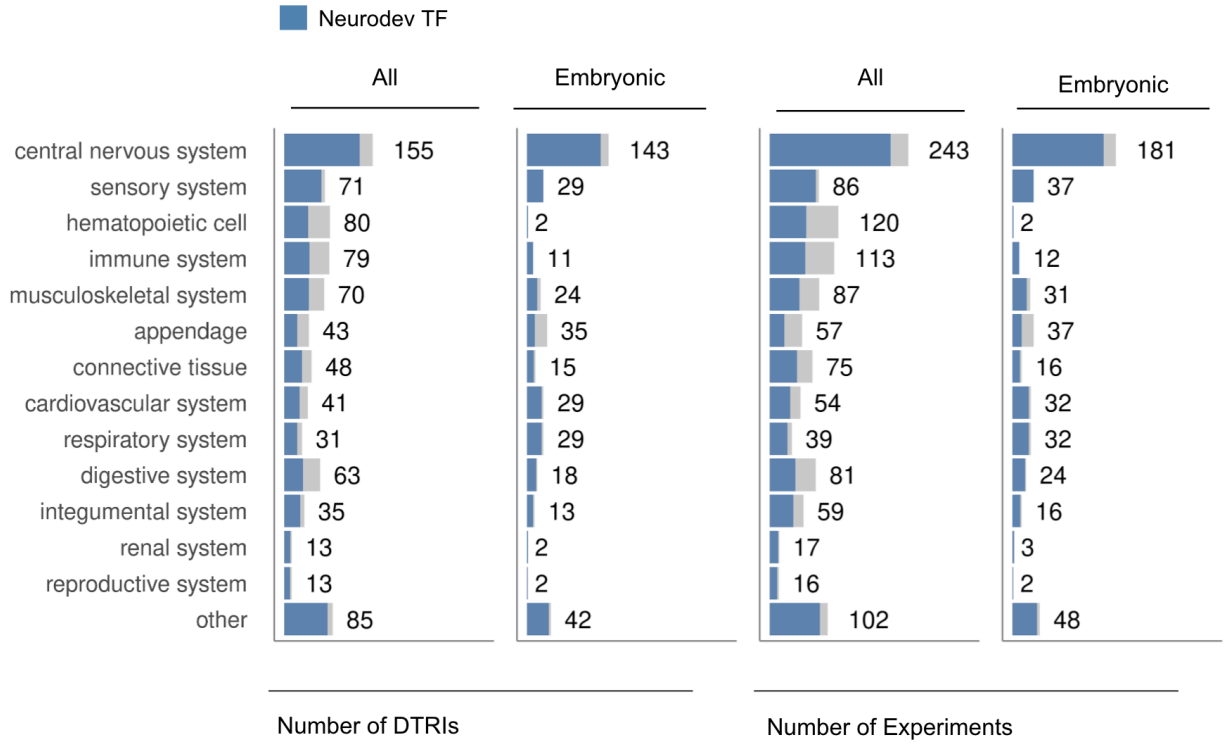

929

930 **Supplementary Figure S7.** Breakdown of experiments performed using primary tissues or cells

931 across anatomical systems.

932 DTRI counts are plotted on the left and experiment counts are plotted on the right. Additional

933 columns are shown for experiments performed using embryonic tissue or cells. DTRIs and

934 experiments involving neurodevelopmental TF regulators are highlighted in blue.

935

936

937

bioRxiv preprint doi: https://doi.org/10.1101/2021.04.11.439248; this version posted April 12, 2021. The copyright holder for this preprint (which was not certified by peer review) is the author/funder, who has granted bioRxiv a license to display the preprint in perpetuity. It is made available under aCC-BY 4.0 International license.

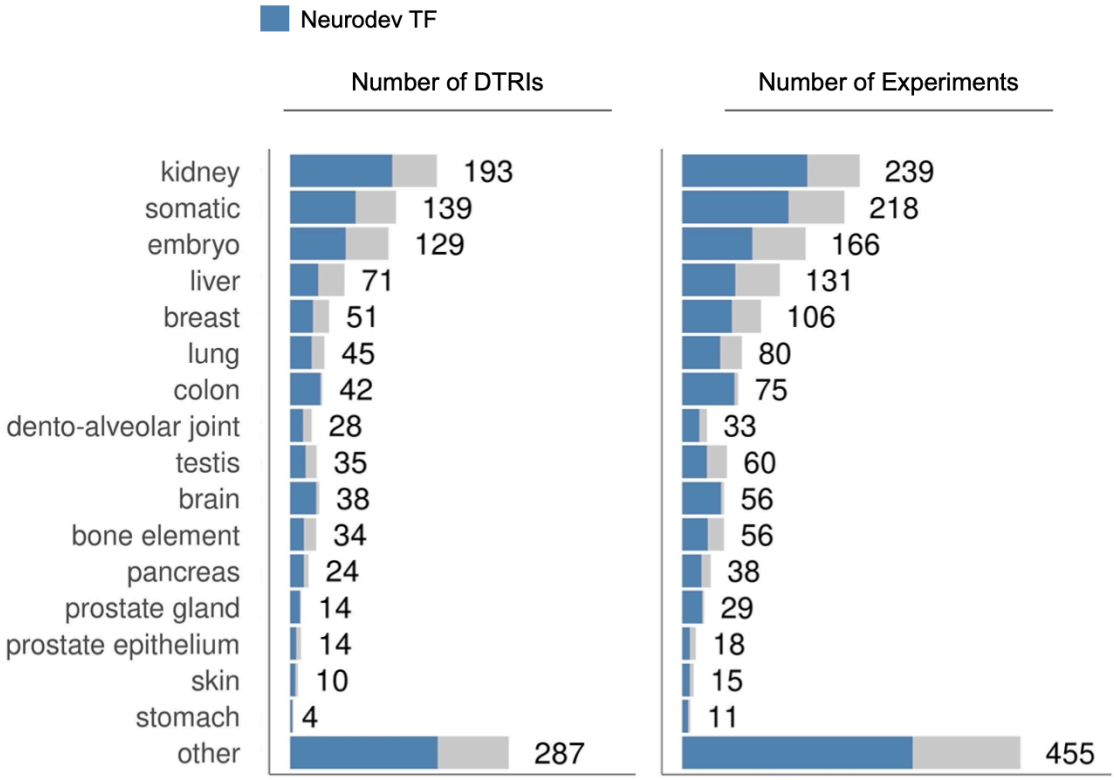

938

939 **Supplementary Figure S8.** Breakdown of experiments performed using cell lines across broad

940 cell type categories.

941 DTRI counts are plotted on the left and experiment counts are plotted on the right. DTRIs

942 involving neurodevelopmental TF regulators are highlighted in blue.

943

944

bioRxiv preprint doi: https://doi.org/10.1101/2021.04.11.439248; this version posted April 12, 2021. The copyright holder for this preprint (which was not certified by peer review) is the author/funder, who has granted bioRxiv a license to display the preprint in perpetuity. It is made available under aCC-BY 4.0 International license.

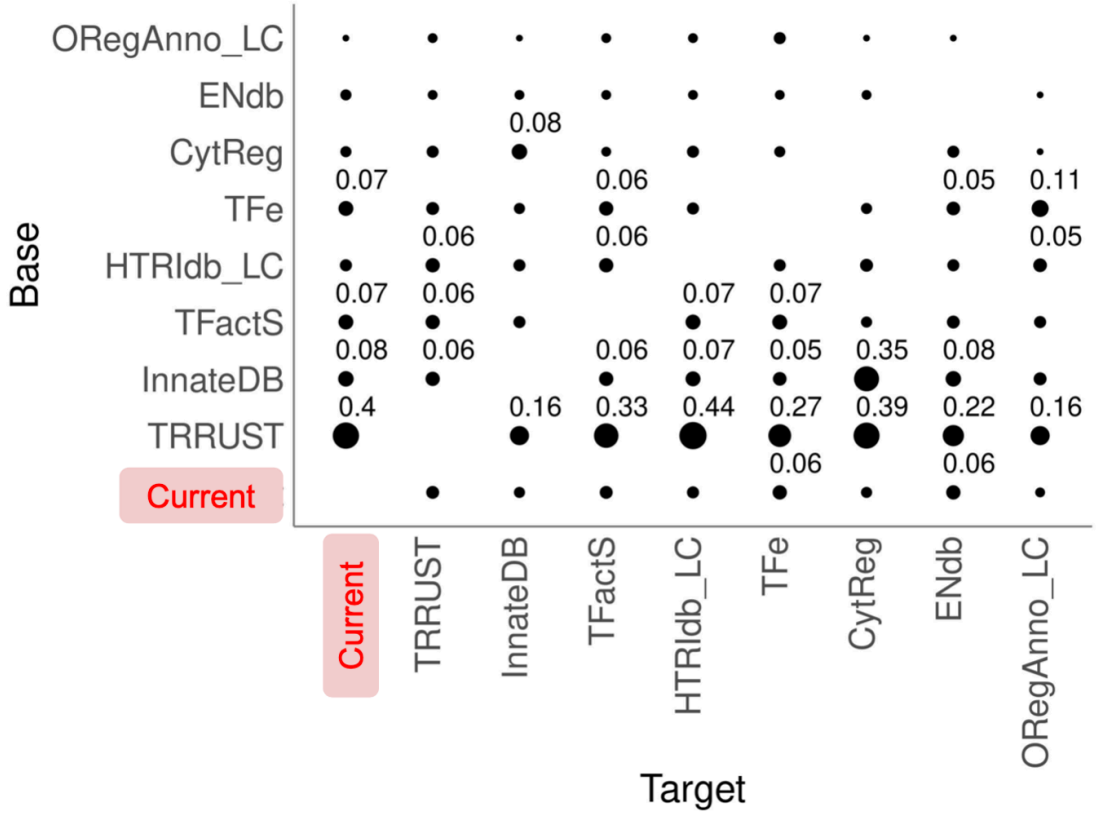

Supplementary Figure S9. Pairwise overlap of DTRIs among the different data resources. Overlap values are reported as fractions of the "target" resource (x-axis). Only values of 0.05 or higher are printed. For example, TRRUST contains 0.4 of the DTRIs recorded in our curation whereas we captured less than 0.05 of the DTRIs in TRRUST. External resources are ordered by the number of recorded DTRIs.

bioRxiv preprint doi: https://doi.org/10.1101/2021.04.11.439248; this version posted April 12, 2021. The copyright holder for this preprint (which was not certified by peer review) is the author/funder, who has granted bioRxiv a license to display the preprint in perpetuity. It is made available under aCC-BY 4.0 International license.

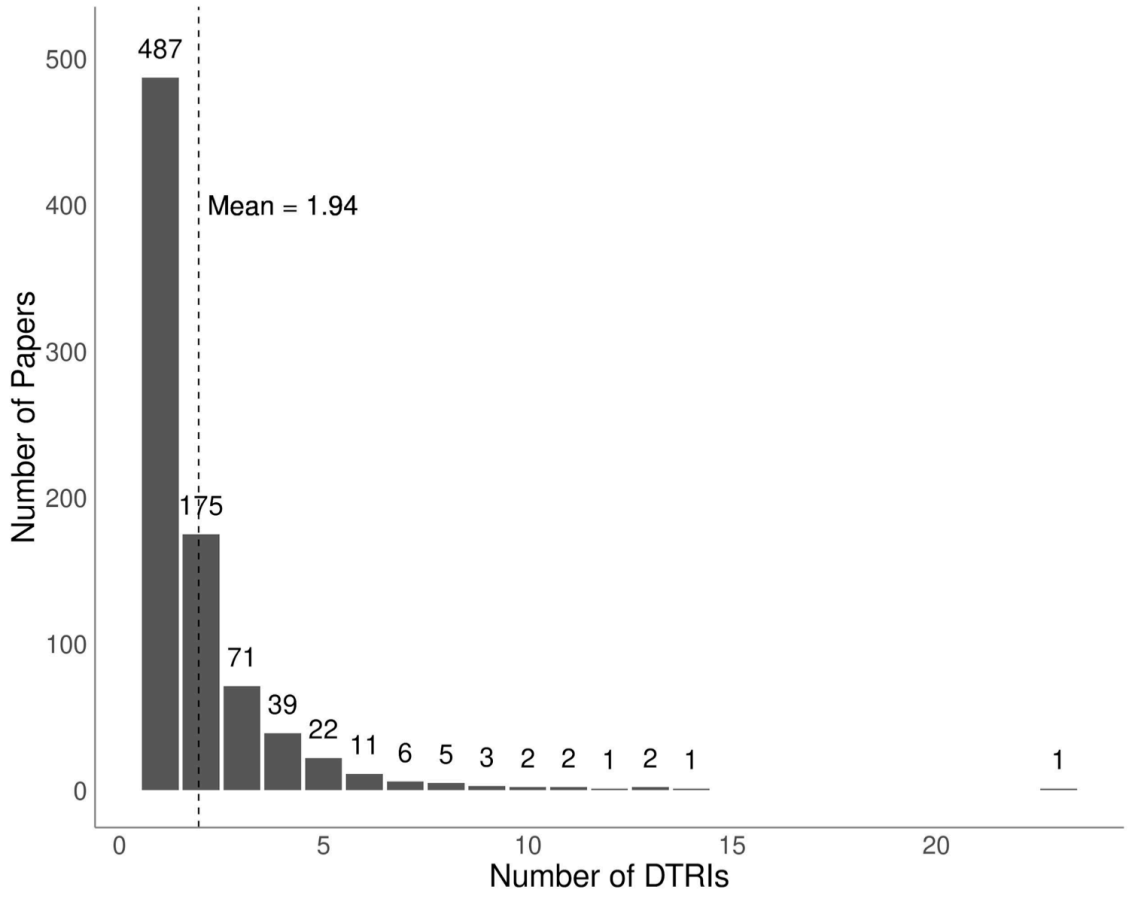

Supplementary Figure S10. Distribution of papers by the number of DTRIs reported. Only papers with at least one curated DTRI are included. The majority of papers report only a single DTRI.

bioRxiv preprint doi: https://doi.org/10.1101/2021.04.11.439248; this version posted April 12, 2021. The copyright holder for this preprint (which was not certified by peer review) is the author/funder, who has granted bioRxiv a license to display the preprint in perpetuity. It is made available under aCC-BY 4.0 International license.

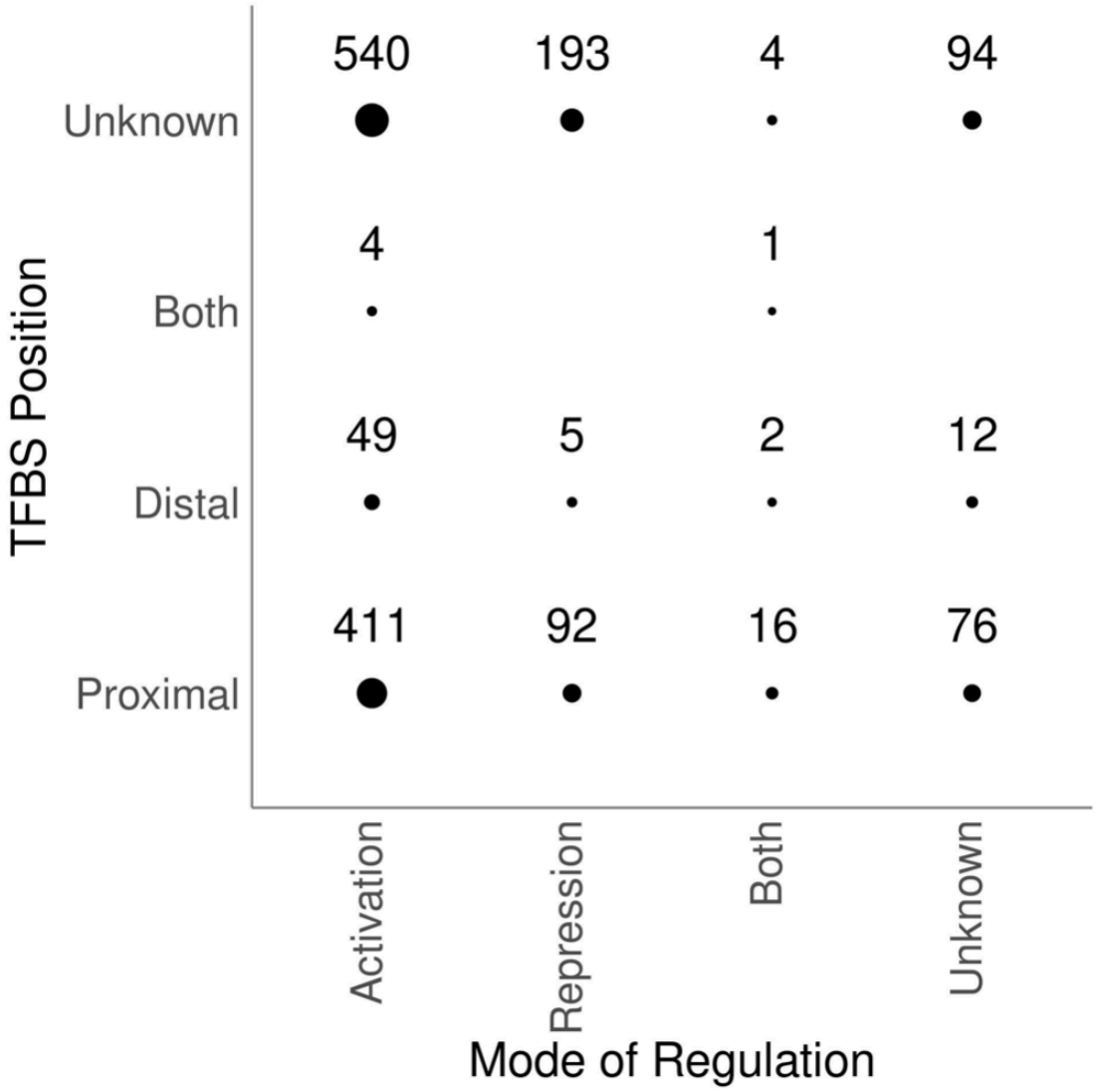

967

968 **Supplementary Figure S11.** Breakdown of DTRIs by mode of regulation and TFBS position.

969 For "TFBS Position" (y-axis), "Proximal" refers to promoters or cREs that are within 3 kb of the

970 target TSS as reported in the original publication. The "Distal" category includes cREs further

971 than 3 kb upstream or downstream from the target TSS. "Both" includes DTRIs with both

972 proximal and distal regulatory elements. For "Mode of Regulation", "Activation" refers to TF

973 perturbation or TF-reporter assays where the direction of change in target gene expression is

974 the same as direction of the corresponding TF perturbation. Similarly, "Repression" includes

bioRxiv preprint doi: https://doi.org/10.1101/2021.04.11.439248; this version posted April 12, 2021. The copyright holder for this preprint (which was not certified by peer review) is the author/funder, who has granted bioRxiv a license to display the preprint in perpetuity. It is made available under aCC-BY 4.0 International license.

975 results where expression of the target gene changes in the opposite direction. “Both” refers to

976 DTRIs with alternative results from different experiments.

977

978

979

980

981

982

983

984

985

986

987

988

bioRxiv preprint doi: https://doi.org/10.1101/2021.04.11.439248; this version posted April 12, 2021. The copyright holder for this preprint (which was not certified by peer review) is the author/funder, who has granted bioRxiv a license to display the preprint in perpetuity. It is made available under aCC-BY 4.0 International license.

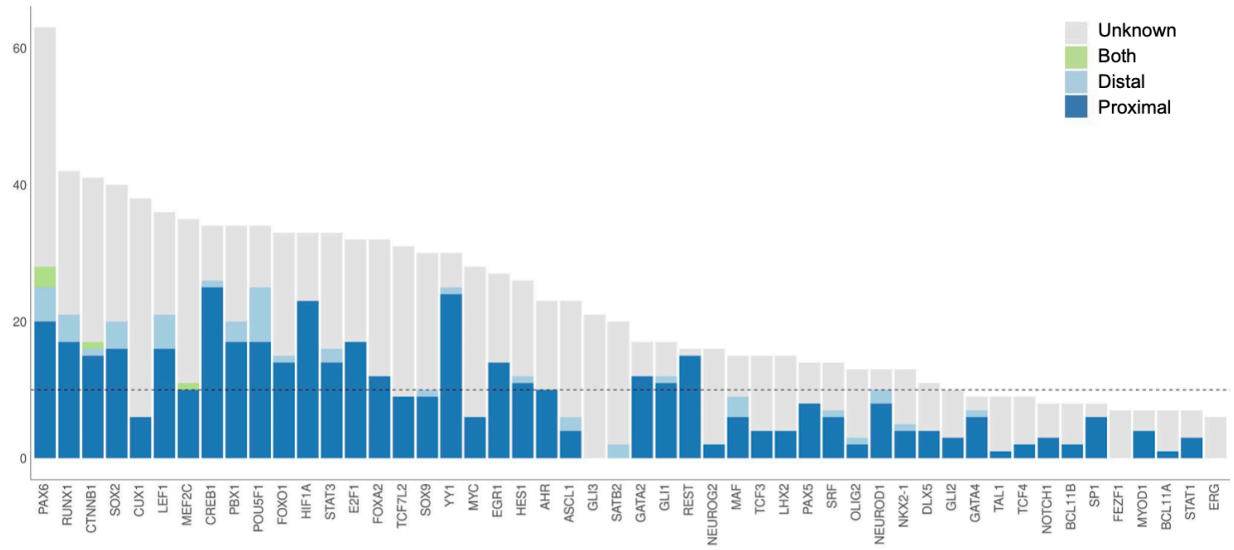

Supplementary Figure S12. TFBS Position of DTRIs per TF for the top 50 TFs. Colors correspond to TFBS position annotations. Dotted line indicates 10 targets on the y-axis for reference.

bioRxiv preprint doi: https://doi.org/10.1101/2021.04.11.439248; this version posted April 12, 2021. The copyright holder for this preprint (which was not certified by peer review) is the author/funder, who has granted bioRxiv a license to display the preprint in perpetuity. It is made available under aCC-BY 4.0 International license.

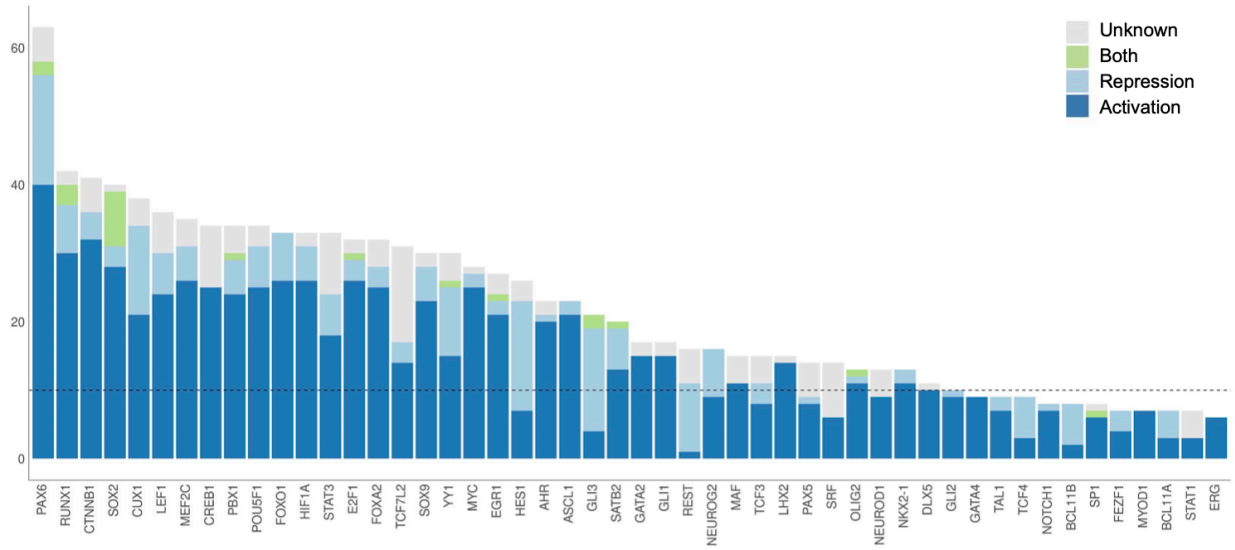

Supplementary Figure S13. Mode of regulation of DTRIs per TF for the top 50 TFs. Colors correspond to the mode of regulation annotations. The dotted line indicates 10 on the y-axis for reference. Most TFs appear to be primarily activators whereas a small number of TFs such as HES1, GLI3, and REST repress the majority of their recorded targets.

bioRxiv preprint doi: https://doi.org/10.1101/2021.04.11.439248; this version posted April 12, 2021. The copyright holder for this preprint (which was not certified by peer review) is the author/funder, who has granted bioRxiv a license to display the preprint in perpetuity. It is made available under aCC-BY 4.0 International license.

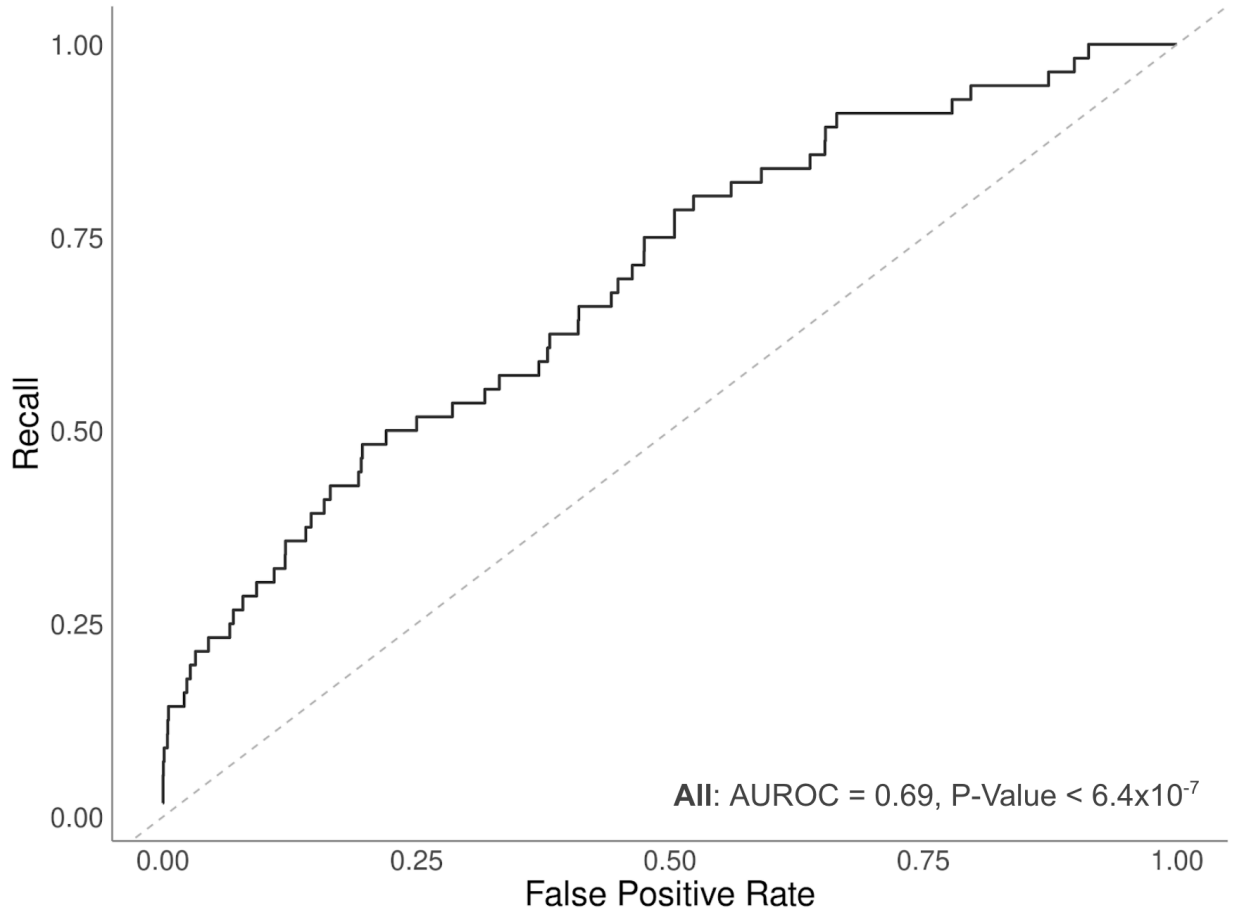

Supplementary Figure S14. Enrichment of all curated PAX6/Pax6 targets among differentially expressed genes in the Pax6 TF perturbation dataset.

AUROC and the corresponding p-value (Mann-Whitney U Test) are displayed in the panel.

bioRxiv preprint doi: https://doi.org/10.1101/2021.04.11.439248; this version posted April 12, 2021. The copyright holder for this preprint (which was not certified by peer review) is the author/funder, who has granted bioRxiv a license to display the preprint in perpetuity. It is made available under aCC-BY 4.0 International license.

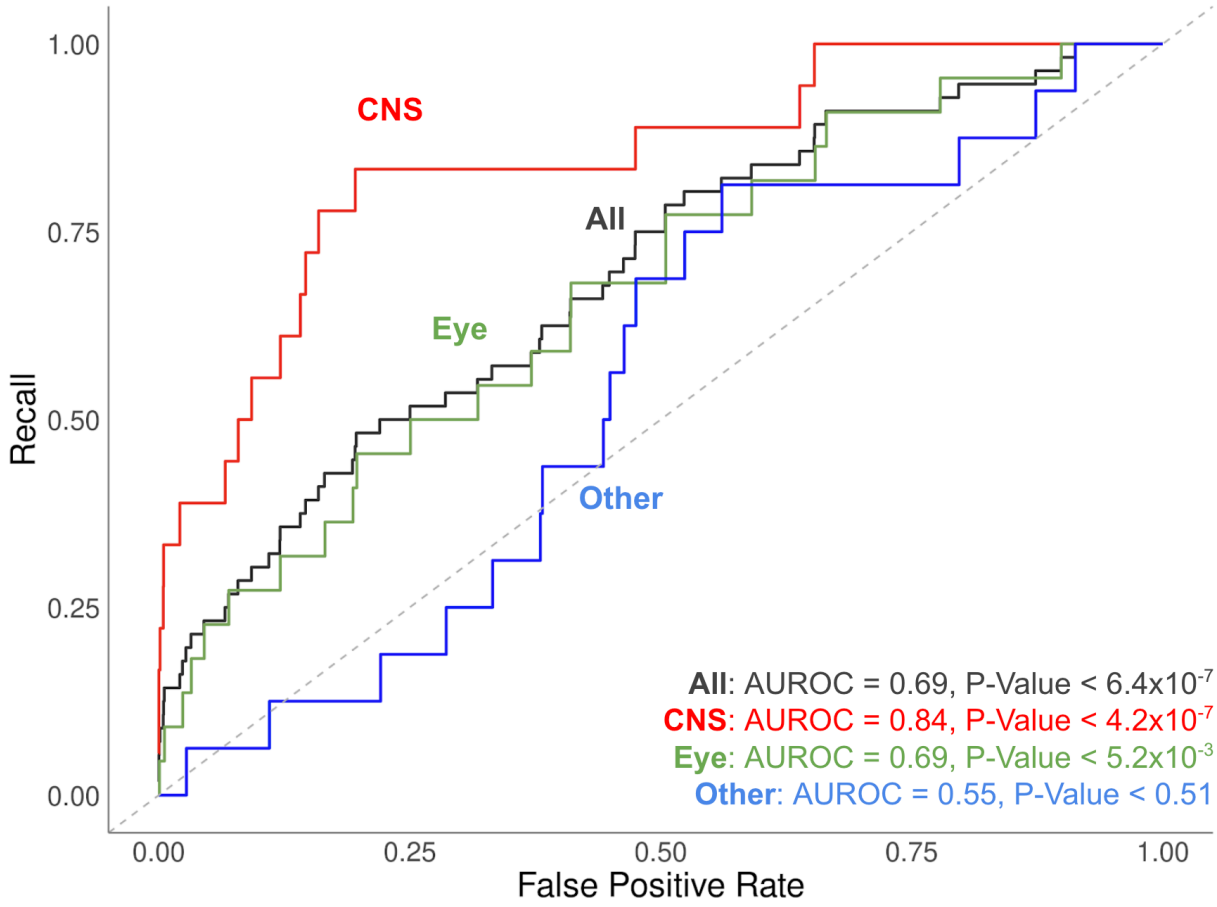

Supplementary Figure S15. Enrichment of curated PAX6/Pax6 targets among differentially expressed genes in the Pax6 TF perturbation dataset by tissue types.

Targets are classified based on the reported cellular contexts. AUROCs and the corresponding p-values (Mann-Whitney U Test) are displayed in the panel. Color coding corresponds to categories of targets. Targets with experimental validation in primary CNS tissues are most enriched in the perturbation screen. No statistically significant enrichment is observed for targets tested in tissues or cell types other than the CNS or the eye.

bioRxiv preprint doi: https://doi.org/10.1101/2021.04.11.439248; this version posted April 12, 2021. The copyright holder for this preprint (which was not certified by peer review) is the author/funder, who has granted bioRxiv a license to display the preprint in perpetuity. It is made available under aCC-BY 4.0 International license.

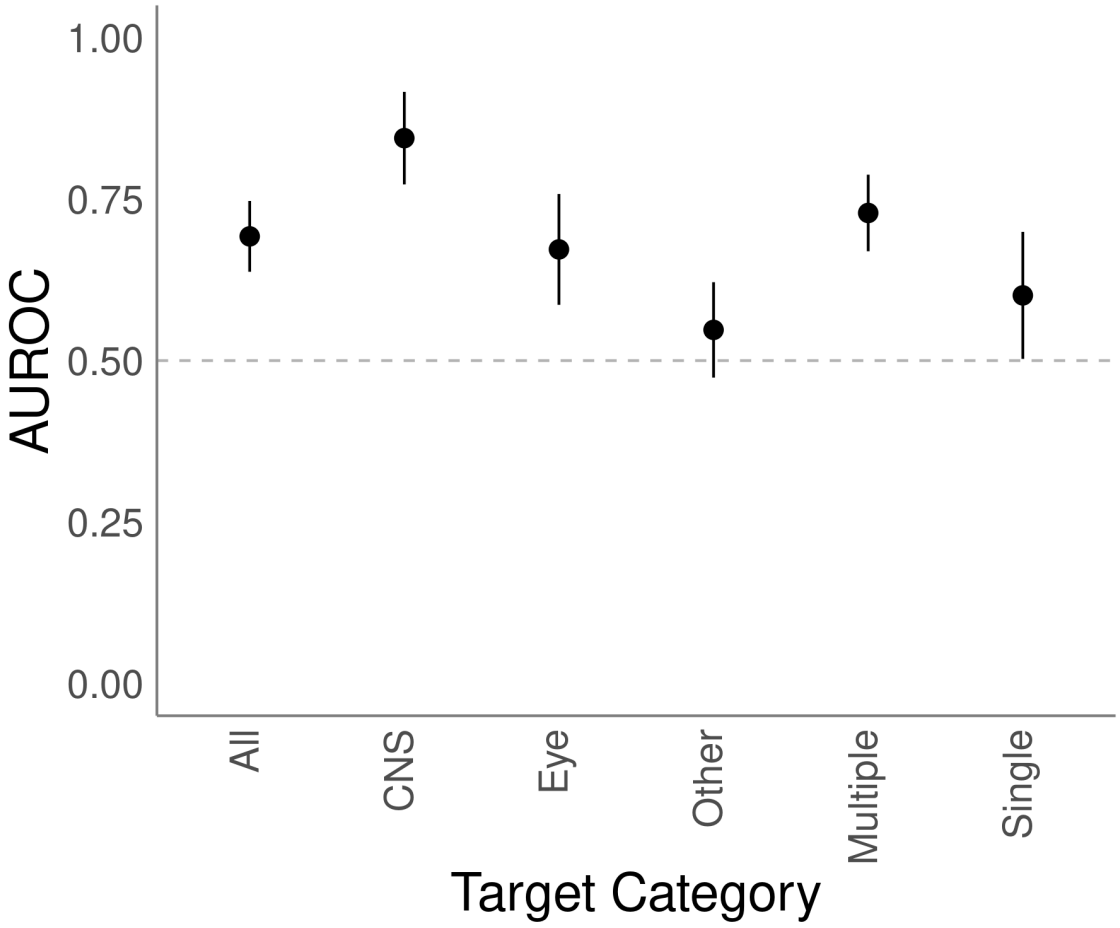

Supplementary Figure S16. AUROC values for the different categories of curated PAX6/Pax6 targets.

Confidence intervals (95th percentile) were derived by bootstrapping 1000 random samples from each category. Statistically significant differences were observed between the CNS versus "other" as well as between targets with multiple versus a single type of low-throughput experimental evidence. Dotted line of AUROC = 0.5 indicates random expectation.

bioRxiv preprint doi: https://doi.org/10.1101/2021.04.11.439248; this version posted April 12, 2021. The copyright holder for this preprint (which was not certified by peer review) is the author/funder, who has granted bioRxiv a license to display the preprint in perpetuity. It is made available under aCC-BY 4.0 International license.

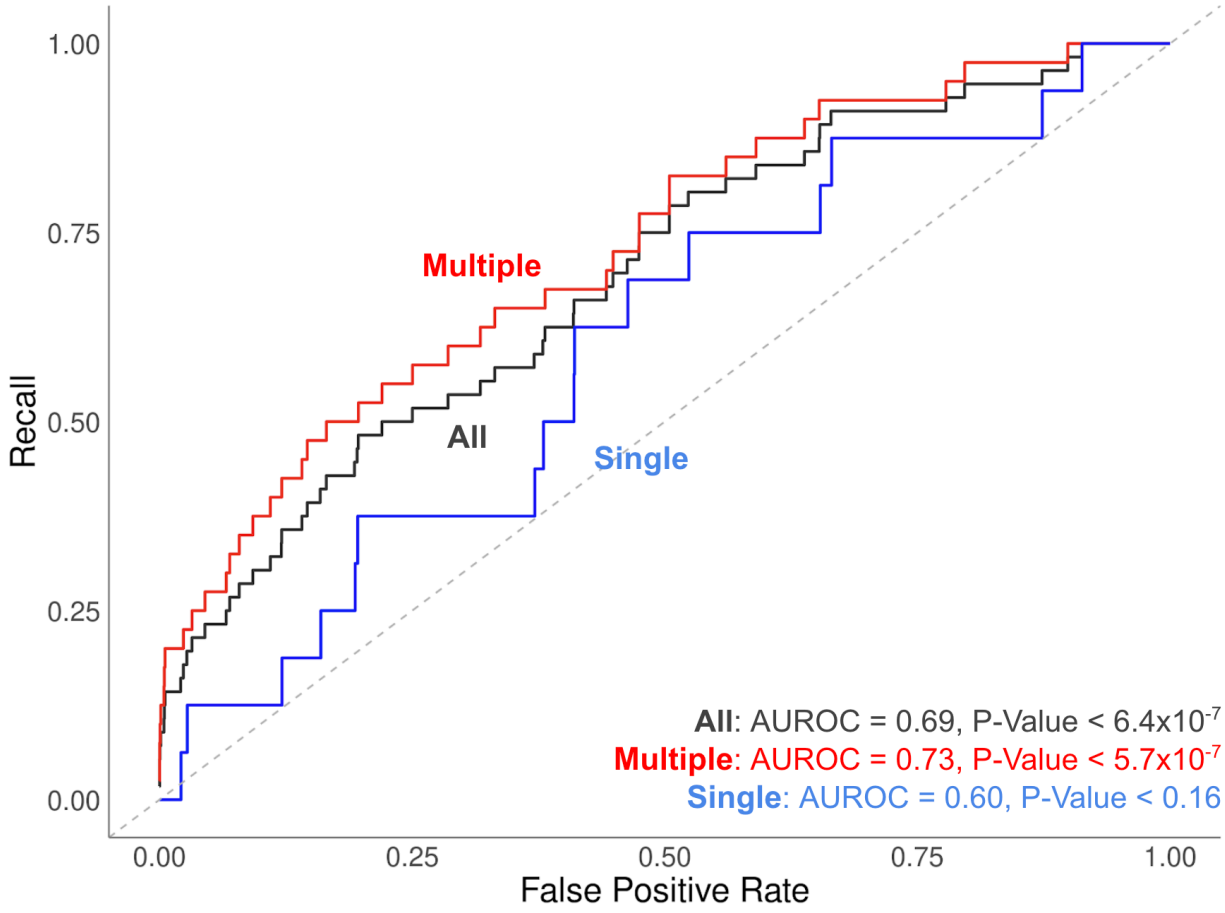

Supplementary Figure S17. Enrichment of curated PAX6/Pax6 targets among differentially expressed genes in the Pax6 TF perturbation dataset.

AUROCs and the corresponding p-values (Mann-Whitney U Test) are displayed in the panel. Color coding corresponds to categories of targets. No statistically significant enrichment is observed for targets tested only in a single type of experiment.